Trinity College Dublin
Coláiste na Tríonóide, Baile Átha Cliath
The University of Dublin

Characterisation of the small regulatory RNA SabS in *Acinetobacter baumannii*

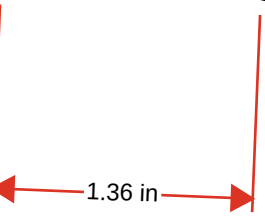

MSc Microbiology, 2026

Ciara O'Sullivan

Supervisor: Carsten Kröger

Moyne Institute of Preventive Medicine

Department of Microbiology

Trinity College Dublin, the University of Dublin

Declaration

I declare that this thesis has not been submitted as an exercise for a degree at this or any other university and it is entirely my own work. I confirm that the work has been completed in full compliance with relevant university policies, including the Academic Integrity policy, the Trinity Policy on Good Research Practice, and the guidance on AI and GenAI in Teaching, Learning, Assessment and Research.

I agree to deposit this thesis in the University's open access institutional repository or allow the Library to do so on my behalf, subject to Irish Copyright Legislation and Trinity College Library conditions of use and acknowledgement. I consent / do not consent to the examiner retaining a copy of the thesis beyond the examining period, should they so wish (EU GDPR May 2018).

Signed: Ciara O'Sullivan

Date: 29/9/25

Acknowledgements

I would like to express sincere thanks to my supervisor – Asst. Prof. Carsten Kröger, who's guidance during my time as a student in the Moyne has been invaluable. Completing this master's has been an incredible learning experience, and I would not have been able to do it without the support of the staff and postgraduate students in the Moyne. I would like to extend particular thanks to Fergal, Rebecca, and Orlaith for their insight and advice — I truly appreciate all the time taken to help me improve my lab technique, and willingness to answer any questions I had, as well as creating such a welcoming environment in the lab. I would like to thank my fellow master's students – Orla, Elizabeth, Weronika and Tapasya – for making every day in the Moyne enjoyable.

Table of Contents

Summary

Acinetobacter baumannii is a Gram-negative nosocomial pathogen, known for its persistence in harsh environments and increasing antibiotic resistance profile. This pathogen is known for its genomic flexibility, and ability to acquire antibiotic resistance determinants through horizontal gene transfer, conjugation, and outer membrane vesicle mediated transfer. Emerging evidence points towards small RNAs (sRNAs) as a mechanism by which bacteria regulate gene expression post-transcriptionally to respond to environmental stressors, however sRNA mediated gene regulation in *A. baumannii* remains poorly understood. The development of pulldown methods coupled with high-throughput sequencing, such as Hi-GRIL-seq has advanced understanding of the sRNA biology of pathogens such as *A. baumannii*. This study focuses on the characterisation of the sRNA SabS, which was shown to be directly regulated at the promoter level by the SigAB sigma factor during copper stress. Previous Hi-GRIL-seq results have identified four putative mRNA targets of SabS: ABUW_RS18870, ABUW_RS00045, ABUW_RS13040, and ABUW_RS15920. During this study these targets were verified *in vivo*, using the pAMCK 2-plasmid reporter system in both *A. baumannii*, and *E. coli*. In addition, the impact of chromosomal *sabS* and *sigAB* deletions on the expression levels of these four mRNAs was tested. The AB5075 *sabS* mutant strain exhibited growth defects when subject to SDS mediated envelope stress, however this phenotype was not observed in the *sigAB* mutant strain, suggesting an independent role of SabS in mediating envelope stress. Furthermore, Hi-GRIL-seq analysis carried out at early stationary phase uncovered several putative sRNA-containing chimeras, as well as the previously validated interaction between SabS and ABUW_RS00045.

Introduction

Acinetobacter baumannii (A. baumannii) is a Gram-negative ESKAPE pathogen, belonging to the *Moraxellaceae* family. The genus Acinetobacter encompasses bacteria with Gram-negative, non-fastidious, oxidase negative, catalase positive and non-glucose fermenting properties. In recent years, *A. baumannii* has gained global significance as a pathogen of increasing antibiotic resistance. The primary antibiotic resistance mechanisms include alteration of the antibiotic target site, controlling antibiotic movement through membranes and efflux pumps, and enzymatic secretion to neutralize antibiotics(Kyriakidis et al., 2021).

Epidemiology and clinical relevance

The rise of antibiotic resistant pathogens is posing a challenge for healthcare systems, as many first line antibiotics are becoming ineffective with the steady increase of multi-drug resistant (MDR) pathogens. In addition, the drug development pipeline is declining, further contributing to the crisis (Miller & Arias, 2024). *Acinetobacter* is now classed as one of six ESKAPE pathogens (*Enterococcus faecium, Staphylococcus aureus, Klebsiella pneumoniae, Acinetobacter baumannii, Pseudomonas aeruginosa,* and *Enterobacter* species). ESKAPE pathogens are designated as such by the Centers of Disease Control (CDC) due to their increasing resistance to last-line antibiotics and persistent infections in nosocomial settings. *A. baumannii* is notable for its ability to persist in hospital environments and develop resistance to antimicrobials (Lin, 2014), and its designation as a WHO Bacterial Priority Pathogen, in the "critical priority" category (Sati et al., 2025). It primarily infects immunocompromised individuals and as such has become prevalent in hospital environments (McConnell et al., 2013). Infections are often severe, invasive and linked with high mortality rates, as well as a range of disease outcomes, including but not limited to: hospital acquired and ventilator acquired pneumonia (HAP/VAP), urinary tract infections, meningitis, bacteremia, and gastrointestinal and skin/wound infections (Kyriakidis et al., 2021).

Virulence Factors

A. baumannii possesses a range of virulence factors that enhance pathogenicity and mortality, and aid in its ability to persist in stressful conditions (Dehbanipour & Ghalavand, 2022; Harding et al., 2018). A significant virulence factor is OmpA, an outer membrane protein (OMP) that has been implicated in its virulence by binding to host epithelia and mitochondria and causing cell apoptosis. OmpA is a highly abundant surface protein on the pathogen and has been shown to be involved in complement resistance and formation of biofilms (Lucidi et al., 2024). This ability of *A. baumannii* to form biofilms enables it to persist in unfavorable environments, including abiotic surfaces. Biofilm formation can be mediated by pili assembly, and production of biofilm-associated protein (Bap). Pili mediate attachment to abiotic surfaces and formation of microcolonies, preceding the formation of mature biofilm structures. BAP proteins are expressed on bacterial cell surfaces and enhance biofilm formation on abiotic or biotic surfaces. The formation of biofilms mediated by Bap or pilin proteins can be influenced by environmental signals such as metal cations. (Howard et al., 2012).

Antimicrobial Resistance Mechanisms of *A. baumannii*

Antibiotic hydrolyzing enzymes

The production of antibiotic hydrolyzing enzymes is a common mechanism of resistance in many Gram-negative bacteria, including *A. baumannii*. Of note, *A. baumannii* exhibits intrinsic resistance to β-lactam antibiotics. β-lactams function by binding to and inactivating penicillin binding proteins (PBPs), thereby disrupting cell wall synthesis and leading to cell death. β-lactamases, enzymes that hydrolyze the β-lactam ring of antibiotics, confer carbapenem resistance in *A. baumannii.* Notable β-lactamases are class B enzymes, known as metallo-β-lactamases or class D enzymes known as oxacillinases. Carbapenem-hydrolyzing class D β-lactamases (CHDLs) are now commonly found in *A. baumannii* and are associated with carbapenemase activity. These enzymes are represented by three groups which are resistant to clavulanic acid and can be either chromosomally or plasmid encoded: OXA-23, OXA-24 and OXA-28. From the 1980s onwards, a hallmark of carbapenem resistance in *Acinetobacter* species was the plasmid encoded β-lactamases enzymes, found increasingly in clinical isolates

(Evans & Amyes, 2014). In addition to β-lactamases, *A. baumannii* exhibits aminoglycoside resistance through production of aminoglycoside-modifying enzymes (AMEs), and 16S rRNA methylases. AMEs - including acetyltransferases (AACs), nucleotidyltransferases (ANTs), and phosphotransferases (APHs) - are located either on the bacterial chromosome or on plasmids. Expression of aminoglycoside modifying enzymes results in the alteration of the hydroxyl or amino groups, reducing affinity of the antibiotic for its target site. 16S rRNA methylases have been shown to confer resistance through direct modification of the aminoglycoside target side on the ribosome. Activity of these enzymes is associated with resistance to all clinically relevant aminoglycosides, and genes are often located on transferable plasmids, facilitating horizontal spread (Doi & Arakawa, 2007).

Altered permeability and efflux.

A. baumannii exhibits antibiotic resistance through expression of chromosomally encoded efflux pumps. These reduce the accumulation of antibiotics within the cell, and often work in combination with other resistance mechanisms such as β-lactamase expression. The most clinically relevant are members of the resistance-nodulation-division (RND) superfamily. The AdeABC efflux pump was the first identified in *A. baumannii*, and consists of the AdeA membrane fusion protein, the AdeB transporter, and the AdeC outer membrane factor. Overexpression of the AdeABC efflux pump is regulated by the AdeRS two-component system, and typically confers multidrug resistance (MDR). Its main substrates are aminoglycosides, β-lactams, fluoroquinolones, tetracyclines, tigecycline, macrolides, chloramphenicol and trimethoprim, and expression is frequently associated with clinical isolates. Notably, correlation between overexpression of AdeABC and decreased susceptibility to tigecycline has been found in MDR clinical isolates (Coyne et al., 2011). In addition, *A. baumannii* can acquire carbapenem resistance through porin or penicillin binding protein modifications. Of note is the CarO porin which has been linked to carbapenem resistance (Poirel & Nordmann, 2006).

Horizontal gene transfer and genetic plasticity

In particular, *A. baumannii* is known for its genomic plasticity - aiding in its ability to rapidly acquire mutations, rearrangements and integrate foreign genetic determinants, carried by mobile genetic elements (Kyriakidis et al., 2021). *A. baumannii* frequently acquires resistance determinants through horizontal gene transfer (HGT). This ability, coupled with the selective pressure of hospital environments has contributed to the emergence of extensively drug-resistant (XDR) and pan-drug resistant strains (Sharma & Lakhanpal, 2025). *A. baumannii* utilizes all four known mechanisms of horizontal gene transfer: conjugation, natural transformation, transduction, and outer membrane vesicle (OMV) mediated transfer. Initially, the *bla*$_{OXA}$ genes - encoding for class D β-lactamases - were present in *Acinetobacter resistans* strains and are now found widely in *A. baumannii* isolates. HGT of *bla*$_{OXA}$ genes via plasmid conjugation between *A.baumannii* and *A. baylyi* have been experimentally demonstrated, showing the potential for transmission of resistance genes between strains. In addition, phage mediated transduction between *A. baumannii* strains has been suggested aid in the spread of carbapenemase encoding genes between *A. baumannii strains* (Da Silva & Domingues, 2016). *A. baumannii* also contains a variety of mobile genetic elements which facilitate spread of resistance genes from plasmid to chromosome within the cell. Insertion sequences are short transposable elements, often found upstream of antibiotic resistance elements. They can induce overexpression of antibiotic resistance genes, and are considered major contributors in the genetic plasticity of *A. baumannii.* Examples include the ISAba1 and ISAba125 which can drive expression of class C β-lactamases. *A. baumannii* has shown enhanced expression of intrinsic β-lactamases in the presence of the ISAba1 insertion sequence, as well as enhanced resistance to 3rd generation cephalosporins. Resistance genes flanked by insertion sequences, including β-lactamases are mobilized by transposons such as Tn2006 and Tn125, facilitating the spread of these resistance genes between plasmids and chromosomes (Da Silva & Domingues, 2016; Kyriakidis et al., 2021). In addition, the ISAba13 insertion sequence has shown to mediate phase switching between an avirulent non-capsulated state, and a virulent capsulated state (Whiteway et al., 2022). Furthermore, it has been demonstrated that *A. baumannii* mediates DNA transfer through outer membrane vesicles (OMVs). While this

mechanism of resistance gene dissemination is not well reported, OMV mediated transfer of β-lactamases genes has shown to result in carbapenem resistance in previously susceptible strains (Whiteway et al., 2022).

Post-transcriptional regulation by sRNAs

Small RNAs (sRNAs) are short RNA molecules approximately 50-250 nucleotides in length. They have been identified in a wide range of bacterial species and have shown to be key regulators of gene expression. sRNA expression is often influenced by changing environmental conditions, and can be induced by stressors (Gottesman & Storz, 2011). Bacterial sRNAs primarily regulate gene expression by antisense base pairing with target mRNAs. sRNAs are typically categorised into two groups: *trans*-encoded and *cis*-encoded. *Trans*-encoded sRNAs regulate a target mRNA by base pairing with limited complementarity and are encoded at a separate location in the genome. They are frequently transcribed from intergenic regions (IGRs), or from the 5' or 3' untranslated regions (UTRs) of protein coding genes (Waters et al 2009). These sRNAs often utilise a conserved "seed" region — a short, contiguous row of nucleotides that mediates initial recognition to bind to their target mRNA. *Trans*-encoded sRNAs often base pair with the 5' UTR of the mRNA target and sequester the ribosome binding site, thus preventing translation. In addition, they can initiate RNase mediated degradation of the sRNA-mRNA duplex. Conversely, they can prevent the formation of inhibitory structures that would typically sequester the ribosome binding site, thus allowing for translation of the mRNA. Unlike *cis*-encoded sRNAs, *trans*-encoded sRNAs show little correlation with the chromosomal location of their cognate sRNA, and often base pair with several mRNA targets. *Cis*-encoded sRNAs are encoded from the DNA strand opposite ("antisense") to their target RNA molecule and thus share a high level of complementarity. The physiological roles of *cis*-encoded sRNAs is less understood than *trans*-encoded sRNAs, however some have shown to promote degradation of their target or repress translation (Waters & Storz, 2009).

Trans-encoded sRNAs often rely on RNA chaperone Hfq to facilitate binding to their target. Hfq is a hexameric ring protein and is homologous to Sm and Sm-like proteins, which function in processes such as splicing and mRNA decay in eukaryotes (Waters & Storz, 2009).

It contains at least three distinct RNA-binding surfaces. In *Escherichia coli*, the distal face of Hfq binds A rich sequences, primarily within mRNAs, while the proximal face interacts with sRNAs, binding the poly-U tails of their Rho-independent terminators. Hfq protects RNAs from degradation, and assists in base pairing of sRNA-mRNA duplexes. Hfq mediated sRNA-mRNA binding has been suggested through several models, including causing exposure of the sRNA seed region, as well as positioning the seed region near its target mRNA (Hoekzema et al., 2019). Cis-encoded sRNAs are often expressed constitutively, whereas most *trans*-encoded sRNAs are expressed as a response to certain growth conditions. In *E. coli*, trans-encoded sRNAs have been shown to respond to low iron, oxidative stress, outer membrane stress, and changes in glucose concentration. sRNAs can regulate multiple targets, and therefore a single sRNA is thought to globally modulate specific physiological responses, in a similar manner to a transcription factors. Examples include the small RNA RyhbB in *E. coli*, which mediates the downregulation of iron-sulfur cluster containing enzymes under low iron conditions. In addition, sRNAs MicA and RyhbB have shown to repress outer membrane porin proteins in *E.coli* during envelope stress (Waters & Storz, 2009).

Association with antibiotic resistance and virulence

In addition to regulating physiological stress responses, sRNAs have been implicated in AMR and antibiotic tolerance pathways. To cope with antibiotic stress, bacteria respond with specific transcriptome changes, of which many are often mediated at the post-transcriptional level by sRNAs. The small RNA MicF has been shown to repress translation of the OmpF porin in *E.coli*. Deletion of MicF results in increased susceptibility to cephalosporins and norfloxacin, whereas overexpression of MicF results in decreased susceptibility. Another small RNA, GcvB, prevents translation of *cycA* mRNA, a serine transporter that transports D-cycloserine. Absence of this sRNA in *E.coli* results in increased sensitivity to d-cycloserine (Pulvermacher et al., 2009).
The sRNA MgrR, which regulates modification of the cell envelope, influences the susceptibility of *E.coli* to polymyxin B, an antimicrobial peptide. MgrR inhibits the translation of *eptB* mRNA, encoding an enzyme responsible for the addition of phosphoethanolamine to LPS, thus reducing its negative charge. In the absence of MgrR, there is a reduced negative charge on LPS, which leads to decreased polymyxin B binding, increasing resistance (Moon et

al., 2013). Furthermore, transcriptome and proteome analyses have shown induction of sRNAs in bacteria treated with sub-MIC concentrations of antibiotics. In *Salmonella Typhimurium* four sRNAs accumulated after treatment with half the MIC of tigecycline. Deletion of one of these sRNAs (SroA) was accompanied by increased sensitivity to tigecycline, while complementation of SroA restored the resistance phenotype (Yu & Schneiders, 2012)**.**

Role of sRNAs in *A. baumannii*

Until recent years, much of the RNA biology of *A. baumannii* was unknown. One of the first sRNAs identified in *Acinetobacter* species was Aar (amino acid regulator). It was first identified in *A. baylyi* and was found to be induced during iron limitation and osmotic shock. Aar was highly expressed during stationary phase in minimal medium, while complex medium revealed strong expression in exponential growth phase. Overexpression of Aar during stationary phase showed upregulation of seven mRNAs involved in amino acid metabolism in *A. baylyi.* As such, it was predicted that Aar was involved in amino acid metabolism in *A. baylyi* (Schilling et al., 2010). However, in *A. baumannii* Aar was found to regulate the outer membrane porin CarO, and was not involved in amino acid metabolism, highlighting the diverse roles of sRNAs across bacterial species (Hamrock et al., 2024). Using bioinformatic approaches, 31 potential candidate sRNAs were uncovered in *A. baumannii* ATCC17978 (Sharma et al., 2014). The expression of three of these sRNAs was later confirmed by Northern blotting in *A. baumannii* MTCC1425. In addition, distinct sets of sRNAs were differentially expressed across *A. baumannii* strains MTCC 1425, and ATCC 17978, suggesting that sRNA expression in *A. baumannii* is strain specific. Of these three, AbsR25 was found to be differentially expressed in response to varying concentrations of ethidium bromide. Specifically, it was found to be downregulated in high concentrations. Later it was revealed that AbsR25 was a negative regulator of the *abaF* gene, encoding a major facilitator superfamily (MFS) transporter involved in fosfomycin efflux. Inhibition of *abaF* through AbsR25 lowered the MIC of fosfomycin eight-fold, and decreased biofilm formation and virulence in *A. baumannii.* (Sharma et al., 2014) Further identification of novel sRNAs was carried out in *A. baumannii* strain ATCC17978 using differential RNA-seq to predict transcriptional start sites (TSSs) of sRNAs. Using this method, approximately 110 sRNAs were identified, of which 88 are conserved in strain AB5075 (Kröger et al., 2018). RNA-seq also led to the identification of 78 candidate sRNAs in *A. baumannii* AB5075 with high

expression, accounting for >50% of the 20 most strongly expressed genes (Weiss et al., 2016). Thus, sRNA genes account for a much larger proportion of the *Acinetobacter* genome than previously thought. Several sRNAs in *A. baumannii* have also been implicated in antibiotic resistance and tolerance. Studies suggest that sRNAs in *A. baumannii* may regulate biofilm formation, however this needs further exploration. (Álvarez-Fraga et al., 2017; Shenkutie et al., 2023). In addition, a plasmid encoded sRNA SrvS has been suggested to modulate phase switching in *A. baumannii* AB5075 (Anderson et al., 2020).

Characterising sRNA-mRNA interactions

Given their roles in mediation of AMR and bacterial stress responses, it is imperative to characterise sRNAs and identify their mRNA targets. A wide range of experimental methods have been developed to enhance this process. Initial experiments aimed to identify target mRNAs via comparative transcriptome profiling of wild-type strains versus strains with a deletion of the sRNA of interest. Transcriptome profiling was accomplished first via microarrays, and subsequently by RNA sequencing. These methods provided valuable insights into global transcriptomic expression changes however did not distinguish between direct and indirect effects of sRNAs (Hör et al., 2018). To address this limitation, pulldown methods were developed that capture sRNA-mRNA pairs, providing a detailed and mechanistic view of sRNA function. MS2-affinity purification coupled with RNA sequencing (MAPS) involved tagging the sRNA of interest with an MS2 aptamer at its 5' end, and expressing it in bacteria. Following this, the bacterial cytoplasm is extracted, and the tagged sRNA and its interaction partners are extracted using affinity chromatography. Resulting sRNA-mRNA chimeras are sequenced and mapped to the bacterial genome (Carrier et al., 2016). Methods developed to achieve a genome wide analysis of sRNA-RNA interactions include CLASH and RIL-seq, both involving RNA-binding proteins (RBPs). Both methods involve the crosslinking of the relevant RBP with associated RNAs, and purification via affinity chromatography. Interacting RNAs are ligated, and the resulting chimeras are sequenced and analyzed. However, RIL-seq is mostly applicable to Gram-negative bacteria such as *E. coli* due to increased Hfq activity in Gram-negative bacteria compared to Gram-positive bacteria (Georg et al., 2020). Furthermore, RIL-seq and CLASH rely on previous characterisation of RBPs in the organism of interest. Thus, limiting

their use in species such as *A. baumannii* of which the RBPs are less understood. To bypass the need for prior knowledge of RBPs, GRIL-seq (Global sRNA target identification by Ligation and sequencing) was developed. The method utilizes a T4 RNA Ligase expressed *in vivo*, resulting in ligation of proximal RNAs, followed by sequencing of chimeras and mapping to the bacterial genome. Hi-GRIL-seq was developed by removing the enrichment step, instead using deeper sequencing resolution. Hi-GRIL-seq involves ectopic expression of T4 RNA ligase, ligating proximal RNA-RNA pairs. Computational analysis allows for identification of reads that map to separate loci within the genome, thus distinguishing this as an sRNA-mRNA pair (Zhang et al., 2017).

SabS - Discovery and Potential functions

The term 'keystone sRNA' is typically used to refer to regulatory RNAs that interact with numerous mRNA targets in tandem, allowing them to have a broader influence over gene expression. (Gebhardt et al, 2023). Several keystone sRNAs were revealed from the Hi-GRIL-seq dataset, including sRNA90, recently annotated as SabS (SigAb-dependant sRNA) (Bacon et al., 2025). These sRNAs were found to be overrepresented in the chimeras obtained from the Hi-GRIL-seq dataset, indicating functional importance. Specifically, SabS was found to account for 18.89 % of total chimeric reads. Despite this, SabS showed a low TPM (Transcripts per million) value, indicating large regulatory impact despite low expression (Hamrock, 2025). Furthermore, recent experiments have shown that SabS is directly regulated by sigma factor SigAB by binding to the promoter sequence. Direct targets were identified using genome wide scanning of the *A. baumannii* genome for potential sigAB binding sites that matched the -10 and -35 promoter elements. In addition, chromatin immunoprecipitation followed by sequencing (ChIP-seq) was used to detect DNA regions bound by SigAB *in vivo*. The promoter region upstream of SabS matched both criteria, identifying it as a direct transcriptional target of SigAB (Bacon et al., 2025).

Initially it was hypothesised that SigAB was functionally similar to RpoE, the main ECF found in *E. coli,* however recent experiments have shown that sigAB is directly involved in mediating copper stress, contains a distinct regulon, and is *Acinetobacter* specific. (Casella et al., 2017, Bacon et al., 2025). CRISPRi knockdown of both *sabS* and *sigAB* resulted in the same copper

sensitive phenotype, suggesting that SabS contributes to SigAB mediated copper resistance. In addition, out of 17 candidate DNA motifs, *sigAB*, *relA* and *sabS* promoter sequences showed the strongest signal upon SigAB overexpression. As such, the core regulon of SigAB comprises SigAB itself, the stringent response mediator RelA and the small RNA SabS (Bacon et al., 2025).

Aims of this study

The goal of this project was to functionally characterize the small RNA SabS and verify *in vivo* its putative mRNA targets. To achieve this, the pAMCK two-plasmid translational reporter system was used to quantify the fluorescence intensity using an overexpression plasmid carrying SabS and compare this with a control strain. In addition, we sought to identify potential new targets for SabS carrying out a Hi-GRIL-seq experiment in two distinct growth phases.

Materials and Methods

Media

The media used are summarized in **Table 1.1.** Media were prepared using de-ionized water, and all media were sterilized prior to use by autoclaving. Bacterial cultures were grown in lysogeny broth (LB) at 37°C with shaking at 220 rpm. Bacterial strains were grown on L-agar plates supplemented with antibiotics when appropriate. For growth to a specific optical density, a single colony of the desired strain was inoculated in 4 mL of LB and grown for ~16 hours (37°C). This overnight culture was then used to inoculate a 1:1000 dilution in LB.

Table 1.1: Media used in this study.

Medium	Reagent	Concentration
Lysogeny broth (Lennox, L-broth)	Tryptone NaCl Yeast extract	10 g/L 5 g/L 5 g/L
Lennox agar (Lennox, L-agar)	L-broth Agar	— 1.5% (w/v) agar
Mueller Hinton broth (MH broth)	Beef extract Casein hydrolysate Starch	2 g/L 17.5 g/L 1.5 g/L
Mueller Hinton agar (MH agar)	MH broth Agar	— 1.7% (w/v) agar

Bacterial Strains

Bacterial strains used during this study are outlined in **Table 1.2**. Strains constructed during this study were grown from a single colony for ~16 hours in 4 mL L-Broth. Overnight cultures were used to make cryostocks which were stored at -80°C for long-term use. Cryostocks consisted of 30% glycerol and 70% overnight bacterial culture (v/v).

Table 1.2: Strains used in this study.

Species	Strain	Genotype	Resistance	Source
E. coli	TOP10	*F– mcrA Δ(mrr-hsdRMS-mcrBC) φ80lacZΔM15 ΔlacX74 nupG recA1 araD139 Δ(ara-leu)7697 galE15 galK16 rpsL(StrR) endA1 λ–*	—	Invitrogen
A.baumannii	AB5075	wild-type	—	S. Salcedo (Jacobs et al., 2014)
A.baumannii	AB5075	pAMCK14	Apramycin	Kröger lab
A.baumannii	AB5075	pAMCK18	Tetracycline	Kröger lab (Mogre et al., 2025)
A.baumannii	AB5075	*ΔsRNA90::sacB aacC4*	Apramycin	Kröger Lab
A.baumannii	AB5075	*ΔsigAB - pVRL2Z-sigAB:3XFLAG*	Apramycin	Kröger Lab
A.baumannii	AB5075	pVRL2Z - *t4rnl1*	Zeocin	Kröger Lab
A.baumannii	AB5075	pAMCK14-sRNA90	Apramycin	This study
A.baumannii	AB5075	pAMCK18 - ABUW_RS00045	Tetracycline	This study
A.baumannii	AB5075	pAMCK18 - ABUW_RS13040	Tetracycline	This study

A.baumannii	AB5075	pAMCK18 - ABUW_RS18870	Tetracycline	This study
E.coli	TOP10	pAMCK18 - ABUW_RS00045	Tetracycline	This study
E.coli	TOP10	pAMCK18 - ABUW_RS13040	Tetracycline	This study
E.coli	TOP10	pAMCK18 - ABUW_RS18870	Tetracycline	This study
E.coli	TOP10	pAMCK18 - ABUW_RS15920	Tetracycline	This study

Plasmids

Plasmids used in this study are outlined in **Table 1.3**. Plasmids were maintained in *E. coli* strain TOP10, or *A. baumannii* AB5075 cryostocks at -80°C.

Table 1.3: Plasmids used in this study.

Plasmid name	Description	Resistance	Source
pAMCK18	Target expression plasmid used in translational reporter system	Tetracycline	Kröger lab (Mogre et al., 2025)
pAMCK14	High copy overexpression plasmid used in translational reporter system	Apramycin	Kröger lab (Mogre et al., 2025)
pAMCK15	Control plasmid used in	Apramycin	Kröger lab

	translational reporter system		(Mogre et al., 2025)
pAMCK14-SabS	High copy expression of *sabS* for use in translational reporter system	Apramycin	This study
pAMCK18 -ABUW_RS13220	ABUW_RS13220 - sfGFP expression plasmid used in translational reporter system	Tetracycline	This study
pAMCK18 - ABUW_RS15920	ABUW_RS15920 - sfGFP expression plasmid used in translational reporter system	Tetracycline	This study
pAMCK18 -ABUW_RS00045	ABUW_RS00045 - sfGFP expression plasmid used in translational reporter system	Tetracycline	This study
pAMCK18 - ABUW_RS13040	ABUW_RS13040 - sfGFP expression	Tetracycline	This study

	plasmid used in translational reporter system		
pAMCK18 - ABUW_RS18870	ABUW_RS18870 - sfGFP expression plasmid used in translational reporter system	Tetracycline	This study
pVLR2Z-*t4rnl1*	T4 RNA ligase placed under transcriptional control of L-arabinose inducible P_{BAD} promoter	Zeocin	Kröger lab

Isolation of gDNA for use as PCR template

Chromosomal DNA was routinely used as a template for PCR amplification. Briefly, 400µL of an overnight culture was centrifuged at maximum speed for one minute, and the supernatant was discarded. The pellet was resuspended in 200µL of sterile H_2O and boiled at 100°C for 5 minutes. Cells were vortexed to ensure cell wall disruption and centrifuged again at maximum speed for 5 minutes. The supernatant was transferred to a new microcentrifuge tube and one volume of chloroform was added. The mixture was vortexed (30s) to mix the aqueous and chloroform phases, followed by centrifugation at maximum speed (4°C, 10 min). Approximately 75% of the aqueous phase was transferred to a new microcentrifuge tube. DNA purity and concentration were quantified using the Nanodrop™ spectrophotometer (Thermo Scientific). DNA was stored at -20°C for downstream use.

Polymerase Chain Reaction (PCR)

Polymerase chain reactions (PCR) were carried out to amplify specific genomic DNA (gDNA) sequences, as well as plasmid backbones. Genomic DNA isolated from *A. baumannii* strain AB5075 was used as a template. Genomic DNA, primers, and VeriFi™ Polymerase mix (PCR Biosystems), and water was subject to PCR amplification. Primers used for amplification of inserts were designed with ~20bp sequences homologous to the cloning vector. Homologous sequences are denoted in lowercase, while the rest of the primer is denoted as uppercase. Primer sequences used are outlined in **Table 1.4**. PCR component volumes are outlined in **Table 1.5**. PCR cycling conditions are outlined in **Table 1.6.** Amplification of plasmid backbones for SLiCE cloning was carried out using previously isolated plasmids. VeriFi™ Polymerase mix was used for amplification of both plasmid backbones and gDNA. Transformed colonies were screened for the presence of the correct insert within plasmid constructs using colony PCR. Colony PCR was carried out by dissolving a single colony in 20µL of dH_20, and the mixture was boiled (95°C, 15 min). 1µL of this was used as template DNA for PCR amplification. The conditions used for colony PCR are as outlined in **Table 1.7**.

Table 1.4: Primers used in this study.

Gene	**Primer Sequence**	**Primer Function**
SabS (Forward)	gtgagcggataacaagatactgagcacAACAAGGTCGCAGCAACC	Amplification of *sabS*
SabS (Reverse)	gcctttcgttttatttgatgcctctagaGCCACGAAAGCATTATTGTG	Amplification of *sabS*
ABUW_RS15920 (Forward)	actgagcacatgcatAGACCAGTTAGACTGCTC	Amplification of *ABUW_RS15920*
ABUW_RS15920 (Reverse)	agcggatccgctagcAGCGTTAGCAGCAGGAGC	Amplification of

		ABUW_RS15920
ABUW_RS00045 (Forward)	actgagcacatgcatTTTGAAAGGAAACTTCAAACAA	Amplification of *ABUW_RS00045*
ABUW_RS00045 (Reverse)	agcggatccgctagcGCCTGCTTTTCCTAAGAG	Amplification of *ABUW_RS00045*
ABUW_RS13040 (Forward)	actgagcacatgcatTTCATAATCAGAAGATGAATT	Amplification of *ABUW_RS13040*
ABUW_RS13040 (Reverse)	agcggatccgctagcTGCTATAGCTAAATACTTTGGC	Amplification of *ABUW_RS13040*
ABUW_RS18870 (Forward)	actgagcacatgcat GCGAAGATGAACTTTGC	Amplification of *ABUW_RS18870*
ABUW_RS18870 (Reverse)	agcggatccgctagcTACTACAGAGATAAGACC	Amplification of *ABUW_RS18870*
pAMCK14 backbone (Forward)	GTGCTCAGTATCTTGTTATCCGCTCAC	Amplification of pAMCK14 backbone

pAMCK14 backbone (Reverse)	TCTAGAGGCATCAAATAAAACGAAAGGC	Amplification of pAMCK14 backbone
pAMCK18 backbone (Forward)	GCTAGCGGATCCGCTGGCTCCGCTGC	Amplification of pAMCK18 backbone
pAMCK18 backbone (Reverse)	ATGCATGTGCTCAGTATCTCTATCAC	Amplification of pAMCK18 backbone

Table 1.5: Components for PCRs – Amplification of gDNA for downstream use

Component	**Volume**
2x Polymerase Mix (VeriFi™)	25 µL
Template DNA (~100ng/µL)	Varied
Forward Primer (10µM)	1 µL
Reverse Primer (10µM)	1 µL
Water	Varied
Total	50µL

Table 1.6: PCR cycling conditions.

Step	**Temperature (°C)**	**Time**	**Cycles**
Denaturation	95	2 min	1
Denaturation	95	15s	35

Annealing	Varied	30s	35
Extension	72	Varied	35
Extension	72	7 min	1

Table 1.7: Colony PCR cycling conditions.

Step	Temperature (°C)	Time	Cycles
Denaturation	95	10 min	1
Denaturation	95	15s	35
Annealing	55	30s	35
Extension	72	Varied	35
Extension	72	2 min	1

Isolation of Plasmids from Bacterial Strains

Plasmids were isolated from bacterial cultures grown overnight for ~16 hours (37°C, 220 rpm), supplemented with the appropriate antibiotic. Plasmids were isolated using the E.Z.N.A® Plasmid Mini Kit (Omega Bio-Tek). Overnight cultures (4 mL) of the desired strain were pelleted by centrifugation at maximum speed for one minute, and the supernatant was discarded. The resulting pellet was processed according to the manufacture's guidelines. The concentration of purified plasmids was measured using the Nanodrop™ spectrophotometer (Thermo Scientific), and stored at -20°C.

Agarose Gel Electrophoresis

Agarose gel electrophoresis was routinely used to verify successful amplification of PCR products. Agarose gels were made using agarose powder and 1x TAE (40mM Tris-acetate, 1mM EDTA). The solution was melted and mixed with SYBR™ Safe DNA gel stain (Thermo Fisher Scientific) (1:1000 dilution). PCR product was mixed with 6x DNA loading dye ([40% (v/v) glycerol, 60 mM EDTA, 10 mM Tris-HCl (pH 7.6), 0.25% (w/v) bromophenol blue (pH 8.0), 0.25% xylene cyanol FF, and 0.25% Orange G]) prior to loading. Gels were run in 1x TAE

buffer (100V, 30 min). CSL-MDNA-1KBPLUS (Cleaver Scientific) and Hyperladder IV (Bioline) were used to verify the size of the amplicon before downstream use. Gels were visualized using the safeVIEW-MINI2 Blue Light Transilluminator (Cleaver Scientific).

Purification of PCR Products

Verified PCR products were purified using the E.Z.N.A® Cycle Pure Kit (Omega Bio-Tek) as per the manufacturer's guidelines. The concentration of purified products was measured using the Nanodrop™ spectrophotometer (Thermo Scientific), and stored at -20°C.

*Dpn*I restriction digestion

*Dpn*I restriction digest was used after PCR amplification of plasmid backbones to remove hemi-methylated template plasmid DNA. Approximately 1µg of purified plasmid backbone PCR product was mixed with 1µL of Anza™ 10x Buffer, and 1µL of Anza™ 10 *Dpn*I restriction enzyme (Thermo Fisher Scientific). The volume was adjusted to 10µL using sterile water. The solution was incubated at 37°C for 6-8 hours.

SLiCE cloning

Plasmid constructs were obtained using SLiCE cloning (Zhang et al., 2012). Primers for PCR amplification of insert DNA were designed to include ~20 bp homology to the ends of the plasmid backbone sequence. Purified and *Dpn*I digested plasmid backbone and purified insert PCR products were incubated along with SLiC extract and 10x T4 DNA Ligase buffer (37°C, 1 hour). As a control, one reaction was included with no insert DNA. Reaction components and volumes are outlined in **Table 1.8**.

Table 1.8: SLiCE reaction setup.

Component	SLiCE reaction	SLiCE control
T4 DNA Ligase buffer (10x)	1µL	1µL
SLiC extract	1µL	1µL

PCR amplified linearised plasmid	100ng	100ng
PCR-amplified insert DNA	100ng	0ng
Water	To 10µL	To 10µL
Total	10µL	10µL

Preparation of Calcium Competent *Escherichia coli*

Calcium competent *E. coli* strain TOP10 was routinely used for transformation of plasmid constructs. To prepare the cells for heat shock transformation, a single colony of *E. coli* TOP10 was grown overnight at 37°C at 220 rpm in 4 mL of LB. The culture was used to inoculate 50 mL of LB in a 1:1000 dilution. The culture was grown at 37°C with shaking at 220rpm to an OD_{600} of between 0.4 - 0.8. The culture was then centrifuged for 8 minutes (3220 x g, 4°C). The supernatant was discarded, and the pellet was resuspended in 40 mL of 0.1M ice-cold $CaCl_2$. Cells were incubated on ice for 20 minutes, before repeating the centrifugation step as outlined above. The pellet was resuspended in 10 mL of ice-cold 0.1 M $CaCl_2$ + 1.15 mL of 87% glycerol (v/v). Competent cells were aliquoted (300 µL) and stored at –80°C for downstream use.

Transformation of calcium competent *E. coli*

Transformation of competent *E.coli* TOP10 cells with plasmid DNA was performed by heat shock. Competent cells were thawed on ice and ~10ng of plasmid DNA was added. Cells and plasmid DNA were briefly mixed and incubated for 20 minutes on ice. Cells were then heat shocked at 42°C for 2 minutes followed by incubation on ice for 2 minutes. Following this, 800µL of LB was added and cells were incubated at 37°C for 90 minutes. After incubation, cells were centrifuged at 11,000 x g for 1 minute. Approximately 90% of the supernatant was discarded, and the pellet was resuspended in residual medium. Cells were plated on L-agar plates supplemented with the appropriate antibiotic and grown overnight at 37°C.

Preparation of electrocompetent *A. baumannii*

Electrocompetent *A. baumannii* strains were used for transformation of lipoprotein-expressing fluorescent reporter plasmids. AB5075 pAMCK15 and AB5075 pAMCK14-sabS electrocompetent cells were prepared in this study. To prepare competent cells, a single colony of the desired strain was inoculated into 4 mL of LB, and incubated overnight (37°C, 220 rpm). The next day, 50 mL of LB was inoculated 1:1000 from the overnight culture. The inoculum was grown for 24 hours (37°C, 220 rpm). The entire culture was pelleted by centrifugation (10 min, 3220 x g, 4°C). The pellet was resuspended twice in 25 mL sterile 10% (v/v) ice-cold glycerol, and pelleted by centrifugation (10 min, 3220 x g, 4°C) in between. The pellet was resuspended in 1 mL sterile 10% (v/v) ice-cold glycerol and stored in 50 µL aliquots at -80°C.

Transformation of *A. baumannii* by electroporation

Electroporation cuvettes (2-mm gap) were pre-chilled on ice, and previously prepared electrocompetent cells were thawed on ice prior to use. Approximately 25ng of plasmid DNA was mixed with 50 µL of electrocompetent cells in a pre-chilled cuvette. Cells were subject to electroporation at 2.5 kV, 25 µF capacitance, and 100 Ω resistance. In a separate 1.5 mL Eppendorf tube, 1mL of LB medium was added to the mixture. The cells were incubated at 37°C for 1 hour with shaking at 220rpm. Cells were then pelleted, and the supernatant was discarded. The cells were resuspended in ~100 µL of residual liquid before being plated on pre-warmed agar plates. Transformants were grown at 37°C for 24 hours**.**

Measurement of fluorescence

Relative fluorescence (arbitrary units) and optical density at 600nm (OD_{600}) of bacterial cultures were measured on a Synergy H1 Hybrid Multi-Mode microplate fluorometer (BioTek). For kinetic assays, strains were inoculated at a starting OD_{600}= 0.01 in LB supplemented with the appropriate antibiotic in a 96-well plate. Cultures were then grown for 30 hours at 37 °C with continuous orbital shaking, and fluorescence was measured with excitation at 485 nm and

emission at 508 nm at regular intervals. For individual timepoint measurements, a single colony of the desired strain was inoculated in 1 mL of LB , supplemented with the appropriate antibiotics. Cultures were incubated for 30 hours with shaking at 220 rpm at 37 °C. Fluorescence and OD_{600} were then measured as outlined previously.

Relative fluorescence of each strain was calculated as shown below.

$$\text{Relative Fluorescence} = \frac{\text{Fluorescence}_{\text{sample}} - \text{Fluorescence}_{\text{blank}}}{\text{OD}_{600}}$$

Hi-GRIL-seq

For this experiment, AB5075 expressing the pVRL2Z-*t4rnl1* plasmid was used. Cultures were grown overnight on L-agar supplemented with zeocin at 37°C. The next day, a single colony was used to inoculate 25 mL of LB in a 250 mL Erlenmeyer flask and grown at 37°C with shaking at 220 rpm to the desired OD_{600}. Expression of the T4 RNA ligase gene was induced by the addition of L-arabinose to a final concentration of 100mM, followed by incubation for 1 hour at 37 °C with shaking at 220 rpm. The experiment was carried out in three biological replicates. As a control, three additional biological replicates were grown under the same conditions without the addition of L-arabinose. RNA isolation was then carried out as outlined below.

RNA isolation

RNA isolation was carried out using the TRIzol™ method (Kröger et al., 2013). Firstly, an overnight culture was grown by inoculating a single colony in 4 mL of LB broth and grown for ~16 hours. The culture was used to inoculate 25 mL of LB with a 1:1000 dilution in a 250 mL flask and grown at 37°C with shaking at 220rpm to the desired OD_{600}. The culture was then mixed with 2/5 of the culture volume ice-cold 5% (v/v) phenol pH 4.3, 95% (v/v) ethanol (Phenol Sigma order code: P-4682). Samples were then incubated on ice for 15-30 minutes to

stabilize RNA and prevent degradation, and then centrifuged at 3220 x g for 10 minutes at 4°C. The supernatant was discarded, and the pellets were resuspended in the residual liquid. The remaining culture was transferred to a 1.5 mL microcentrifuge tube and centrifuged at maximum speed for one minute. The supernatant was discarded, and pellets were stored at -80°C. The next day, the pellet was thawed on ice , and dissolved in 1 mL of TRIzol by slowly pipetting up and down. The mixture was then transferred to a 2 mL microcentrifuge tube and 400 µL of $CHCl_3$ was added, before mixing for 10 seconds by inverting the tube. The mixture was centrifuged for 15 minutes at room temperature at maximum speed. The aqueous phase was transferred to a new microcentrifuge tube, and 450µl of Isopropanol was added, before mixing by inverting the tube. The mixture was incubated at room temperature for 30 minutes, and centrifuged at room temperature (15-20°C) at maximum speed. The supernatant was removed, and the pellet was washed with 350µL of 70% EtOH by inverting the tube. The mixture was centrifuged for 10 minutes at maximum speed at room temperature. The supernatant was discarded, and the pellet was air-dried at room temperature. The RNA pellet was resuspended ~30µl of RNase-free H_2O by a 5-minute incubation at 65°C, 900rpm on a thermo-shaker, and vortexed 2-3 times in between. RNA concentration was measured using a Qubit™ fluorometer (Thermo Fisher Scientific), and samples were stored at -80°C until DNase digestion.

DNase I digestion

A total of 40µg of RNA was resuspended in 79µL of sterile H_2O and denatured at 65°C for 5 minutes. This was followed by a 5-minute incubation on ice, before addition of 10µL of 10x DNase I buffer containing $MgCl_2$ (Fermentas, EN5021), 1µl SUPERase·In™ RNase inhibitor (20 U/µL ; Ambion, AM2694), and 10µL DNase I (1 U/µL;Fermentas, EN0521). The mixture was incubated at 37°C for 30-45 minutes. The samples were combined with 100µL of Roti-Aqua-P/C/I (Carl Roth GmbH, X985.1) in 2 mL microcentrifuge tubes, and mixed for 15 seconds. The samples were then centrifuged at ~16,000 x g for 12 minutes at 15°C. The upper phase was transferred to a new 1.5 mL microcentrifuge tube. 2.5 Volumes of 30:1 (EtOH: 3M Na-acetate, pH 6.5). 2.5 Volumes (~300 µL) of 30:1 mix (EtOH) Na-acetate, pH 6.5) was added. The solution was then precipitated for at least one hour or overnight at 15°C and centrifuged for at ~16,000 x g at 4°C for 30 minutes. The supernatant was discarded, and the pellet was washed

with 350µL of 75% EtOH before a 10-minute centrifugation at (4°C , ~16,000 x g) The supernatant was discarded and the pellet was air dried, before being dissolved in 40µL of H_2O by a 5-minute incubation (65°C, 900rpm) and vortexed at intervals of ~2 minutes. RNA concentration was measured using a Qubit™ fluorometer (Thermo Fisher Scientific), and samples were stored at -80°C.

Antibiotic Susceptibility tests

The effect of different antibiotics on *A. baumannii* AB5075 wild-type, Δ*sabS*, and Δ*sigAB* was assessed using the Kirby-Bauer disc diffusion method. A single colony of the desired strain was inoculated in 4 mL of Mueller-Hinton (MH) broth, and grown overnight (37°C, 220 rpm). Overnight cultures were diluted to an OD_{600} of ~0.01, using MH broth and used to lawn onto MH agar plates (20 mL/plate). Antibiotic discs were applied using an antibiotic disc dispenser. Plates were incubated overnight at 37°C. Zones of inhibition were determined as the diameter of the clear inhibition zone. Each experiment was carried out using three biological replicates per strain.

Statistical Analyses

All data were analyzed using GraphPad Prism version 10. Data is presented as mean ± SD with individual points for each biological replicate ($n \geq 3$ per condition, unless stated otherwise). Kinetic growth and fluorescence assays were compared using multiple unpaired t-tests at each timepoint with false discovery rate (FDR) correction applied. Single representative time-points were selected and indicated in the figure legends and analyzed using Welch's unpaired t-test. Differences in fluorescence between endpoint measurements was assessed using unpaired Welch's t-tests. In both kinetic and endpoint assays, statistical significance thresholds were defined as follows; ns = not significant; $p \leq 0.05$ (*), $p \leq 0.01$ (**), $p \leq 0.001$ (***), $p \leq 0.0001$ (****). Growth curves were analyzed by calculating area under the curve (AUC) values for each biological replicate over the 24-hour growth period. Statistical analysis was carried out using unpaired t-test between the mean AUC for each strain.

Results

Chapter 1: Characterisation of SabS

SabS interacts with four candidate mRNA targets.

Prior to this study, a Hi-GRIL-seq experiment was conducted to identify potential sRNA-mRNA chimeras by inducing the expression of T4 RNA ligase *in vivo* in *A. baumannii* AB5075.

Four experimental conditions included: iron starvation (DIP), imipenem shock (IMIP),T4 RNA ligase induced, and uninduced conditions. Transcript per million (TPM) values for each condition are outlined in **Table 1.9.** Despite accounting for 18.89 % of filtered chimeric reads in the Hi-GRIL-seq dataset, the sRNA SabS exhibited a relatively low TPM value, suggesting that SabS may act as a global regulator of gene expression (Hamrock, 2025). Hence, this sRNA was selected for further investigation. Candidate mRNAs showing the highest interaction frequency with SabS were chosen for further analysis. Examination of SabS containing chimeras in the Hi-GRIL-seq dataset revealed four putative SabS interaction partners, each with >50 interactions. All four encode for hypothetical proteins of unknown function (Hamrock, 2025). Total SabS containing chimeric reads for each condition is listed in **Table 1.10.**

Table 1.9: SabS TPM values per condition – Hi-GRIL-seq data (Hamrock, 2025).

sRNA	DIP-1	DIP-2	IMIP-1	IMIP-2	IND-1	IND-2	NI-1	NI-2
SabS	3,424.80	3,729.10	1,874.30	2,527.50	3,603.50	3,586.70	4,241.30	1,598.20

Table 1.10: SabS containing chimeras and candidate targets. The number of SabS containing reads is shown across four conditions for each predicted target.

sRNA	Interaction partner	Product	Total Chimeric Reads	NI Chimeric Reads	IND Chimeric Reads	DIP Chimeric reads	IMIP chimeric reads
SabS	ABUW_RS18870	Hypothetical protein	8705	204	3188	2675	2638
SabS	ABUW_RS15920	Hypothetical protein	360	8	120	149	83
SabS	ABUW_RS13040	Hypothetical protein	80	7	22	26	25
SabS	ABUW_RS00045	Hypothetical protein	81	0	30	35	16

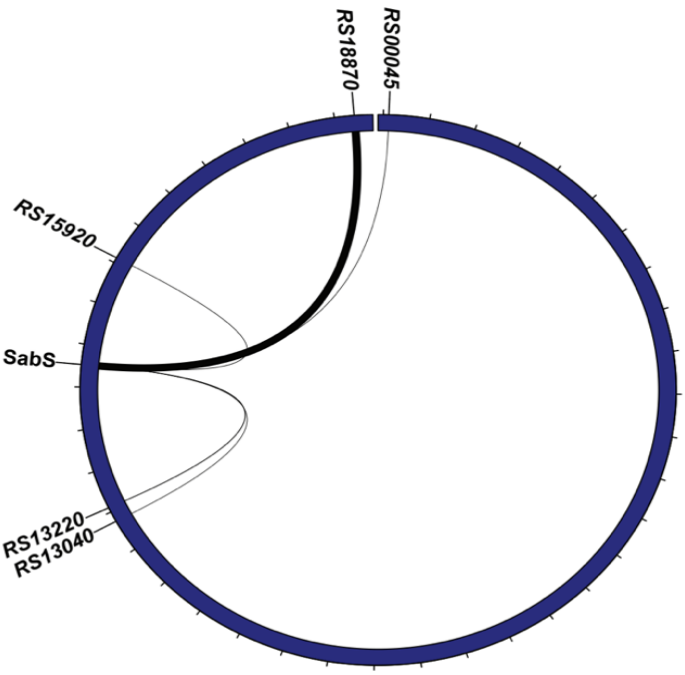

Figure 1.1: Hi-GRIL-seq data shows SabS is ligated with several mRNA targets.

mRNAs found in >50 chimeras with SabS are shown in the circos plot. The circle represents the AB5075 chromosome, with line width corresponding to the number of chimeric sequencing reads.

Predicted interaction sites between SabS and candidate target mRNAs.

The IntaRNA interaction prediction tool was utilized to predict the *in silico* interaction sites between SabS and putative mRNA targets (Busch et al., 2008). IntaRNA predicts base-pairing between mRNA and sRNA sequences, as well as the hybridization energies of each individual interaction. Transcription start sites and terminator sites for target genes were determined from a previously published RNA-seq dataset (Kröger et al., 2018) Primers were designed to amplify the region containing the predicted binding site, which were cloned into a fluorescent reporter plasmid.

IntaRNA was used to predict the likely duplex structures between SabS and its predicted targets. SabS was predicted to form duplexes with ABUW_RS18870 (**Figure 1.2, A)**), ABUW_RS13040, (**Figure 1.2, B)**), ABUW_RS15920 (**Figure 1.2, C)**), and ABUW_RS00045

(**Figure 1.2, D)**). In all cases, base pairing was predicted to occur within the 5'UTR for each target. Hybridization energy for each interaction is shown to the left of each duplex structure, and from -26.49 kcal/mol to -14.63 kcal/mol, indicating these interactions are stable.

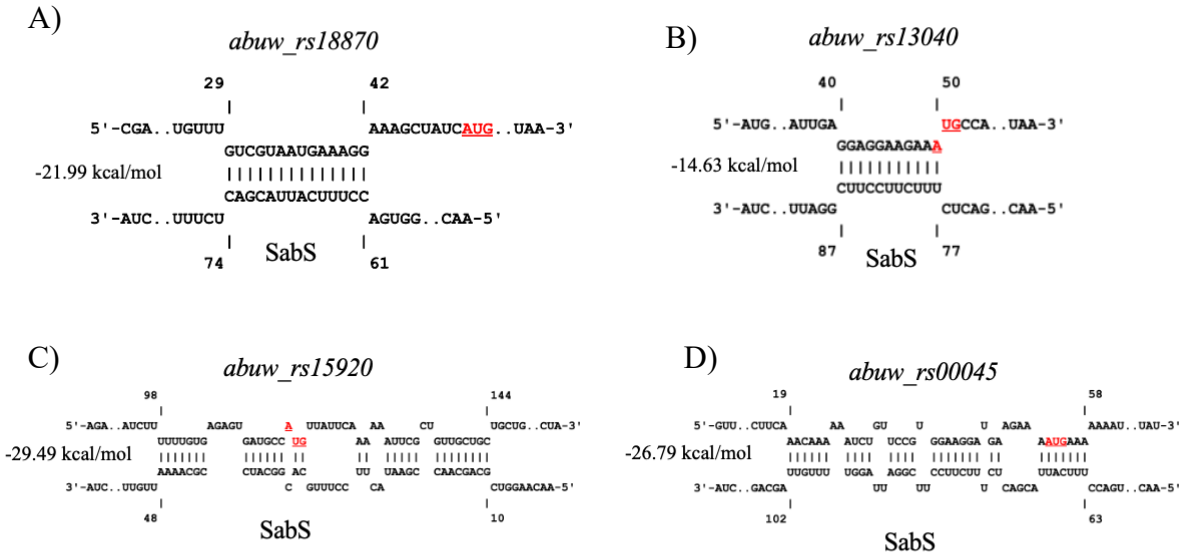

Figure 1.2: IntaRNA predicts SabS - mRNA duplex structures.

IntaRNA predicts the likely duplex structures of sabs and its predicted targets. Start codons are highlighted in red and underlined.

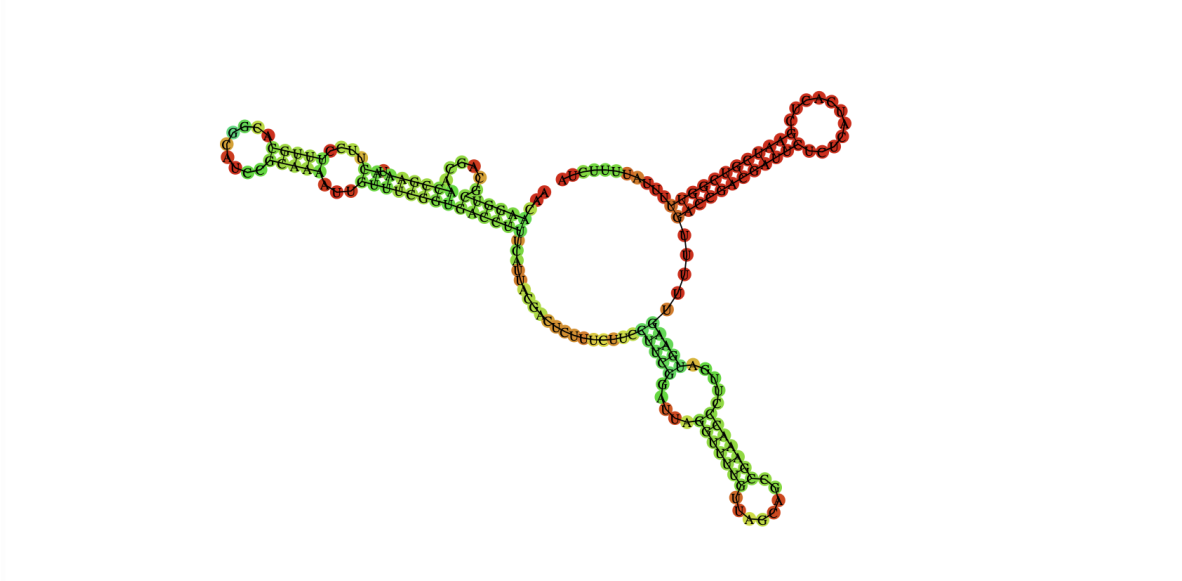

Figure 1.3: RNA fold predicts secondary structure of sabS (MFE = -45.1 kcal/mol)

Colours indicate the base pairing probability, (Red; high, orange/yellow; intermediate, green; low) The secondary structure of SabS was predicted using RNAfold, set to default parameters (Lorenz et al., 2011). SabS was predicted to form a central loop with three stem loop structures protruding from this.

Validating SabS interactions in *A. baumannii* using a two-plasmid reporter system

The original Hi-GRIL-seq experiment outlined previously formed the basis for candidate selection in this study. This experiment involved the enrichment and sequencing of RNA-RNA chimeras that formed *in vivo* under three distinct environmental conditions. Sequencing reads were mapped to the AB5075 genome, and putative sRNA-mRNA interaction pairs were identified by aligning separately the first and last 20 nucleotides of reads that did not map directly to the AB5075. Reads containing an annotated sRNA on one end and a genomic feature on the other end were identified as likely sRNA-mRNA pairs. Of these identified pairs, SabS accounted for 18.89% of total chimeric reads across all tested conditions, suggesting an important functional role in sRNA mediated regulation. Due to its overrepresentation in the Hi-GRIL-seq dataset, SabS was chosen for further investigation, in addition to four hypothetical proteins with high chimeric read counts. While the dataset

suggests interactions between SabS and these hypothetical protein mRNAs, the functional effects of binding on the translation of the target mRNAs were unknown. To investigate this, a two-plasmid reporter system was employed in *A. baumannii* AB5075 (**Figure 1.4).** The system enables analysis of post-transcriptional regulation by an sRNA of interest on a target mRNA, through constitutive overexpression of the sRNA from the plasmid pAMCK14 and the target mRNA as a fusion with *sfGFP* from pAMCK18. Expression of the target mRNA-sfGFP fusion enables quantification of mRNA translation levels based on fluorescence intensity. The two plasmid-reporter system involves the co-expression of the mRNA-sfGFP fusion with either its cognate sRNA or an empty control plasmid. Base-pairing of the mRNA-sfGFP fusion and the sRNA is expected to modulate fluorescence levels relative to the control. Increased fluorescence in the presence of the sRNA-containing plasmid indicates upregulation of the target by the sRNA, while decreased fluorescence indicates translational repression. To validate the interactions between SabS and the hypothetical lipoprotein mRNA targets identified in the Hi-GRIL-seq dataset, this two-plasmid system was employed. Two-plasmid systems have been previously used to characterize sRNA-mRNA interactions in *E. coli* and *S. enterica*, however until recently have not been compatible with co-replication and selection in *A. baumannii* (Mogre et al., 2025).

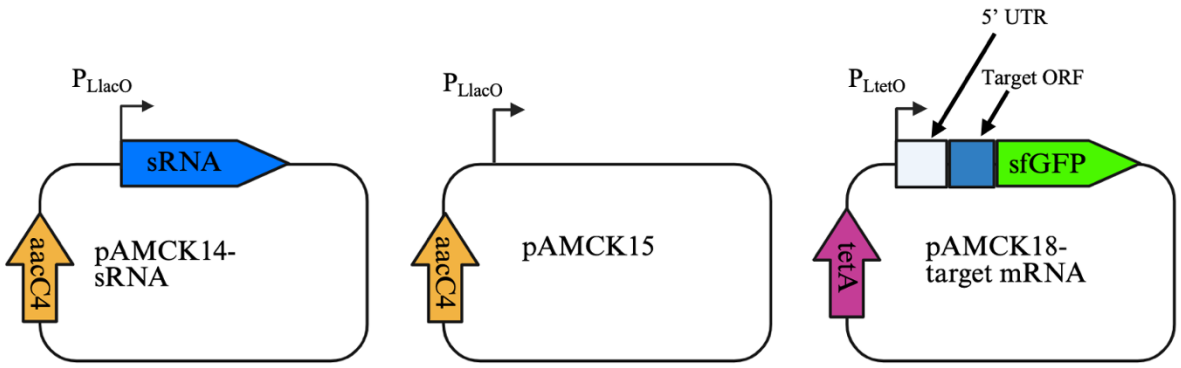

Figure 1.4: Schematic of the two-plasmid reporter system used to analyse sRNA-mRNA interactions.

The sRNA of interest is constitutively over-expressed from the P_{LlacO} promoter on plasmid pAMCK14. pAMCK15 serves as a control plasmid and expresses a small, non-sense RNA. pAMCK14 and pAMCK15 plasmids both contain the aacC4 gene conferring apramycin resistance. pAMCK18 contains a translational fusion of the mRNA target gene with a start-codon-less sfGFP. The mRNA-sfGFP fusion protein is expressed from the P_{LtetO} promoter. The plasmid contains the tetA gene conferring tetracycline resistance. Diagram adapted from (Mogre et al., 2025).

To assess the post-transcriptional impact of SabS on candidate targets, *sabS* was cloned into pAMCK14 and co-expressed with individual pAMCK18-target reporters in *A. baumannii* AB5075. The 5'UTR and first few codons of each candidate target mRNA was cloned into pAMCK18. Each strain was compared with a control strain carrying the corresponding pAMCK18-target construct and the empty pAMCK15 plasmid. Relative fluorescence (AU) and optical density at 600nm (OD_{600}) of each AB5075 pAMCK18-target - pAMCK14-sabs strain was measured by kinetic growth assays and individual timepoint measurements. Expression of sabS significantly reduced relative fluorescence of ABUW_RS18870-sfGFP ($p < 0.05$) in kinetic measurements taken at hour 19 (**Figure 1.5**, **Figure 1.6, A)**) , and in endpoint measurements taken at 30 hours ($p < 0.01$)) (**Figure 1.6, C)**). In addition, Sabs expression significantly enhanced fluorescence intensity of ABUW_RS00045-sfGFP ($p < 0.01$) in kinetic

measurements taken at hour 20 (**Figure 1.5**, **Figure 1.6, A)**), and endpoint measurements taken at 25 hours (**Figure 1.6**, **B)**). There was no significant effect of SabS expression on the relative fluorescence of ABUW_RS13040-sfGFP across kinetic or endpoint measurements. (**Figure 1.5**, **Figure 1.6, A),B),C)**).

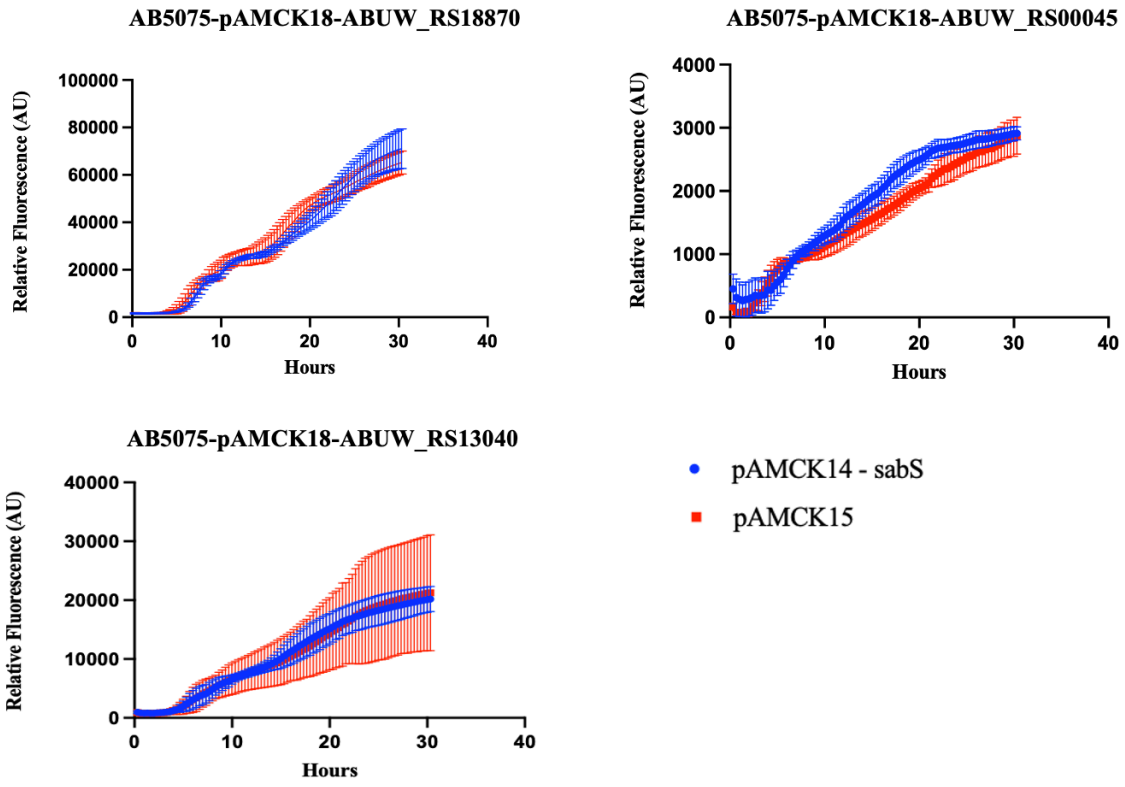

Figure 1.5: Relative fluorescence of AB5075 reporter strains over 30 hours.

AB5075 strains carrying pAMCK18-target were co-expressed with either pAMCK14 – SabS or pAMCK15. Cultures were inoculated from a starting OD_{600} of 0.01 and grown for 30 hours in 96 well plates. Fluorescence and OD_{600} measurements were taken at regular intervals. Data is shown as mean ± SD with individual points for each biological replicate (n ≥ 3 per condition). Strains were compared using multiple t-tests with FDR correction.

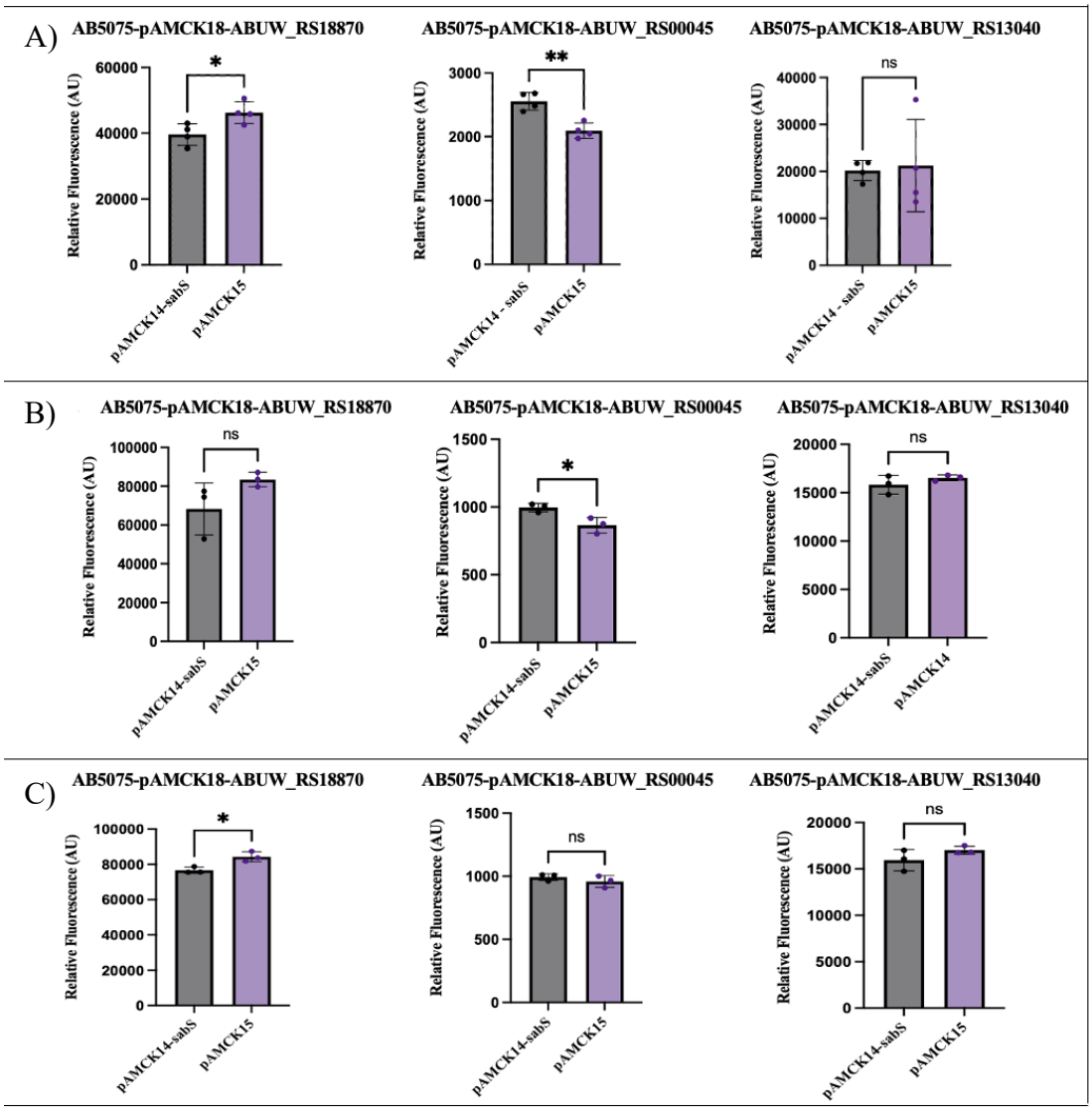

Figure 1.6: Relative fluorescence of AB5075 reporter strains.

AB5075 strains co-expressing pAMCK14-SabS and pAMCK18-target, were cultured in 96 well plates at a starting OD_{600} of 0.01 with measurements of fluorescence and OD_{600} taken at regular intervals. Each strain was compared with a control strain carrying pAMCK14-Sabs and pAMCK15. Data is shown as mean ± SD with individual points for each biological replicate (n ≥ 3 per condition). ns = not significant; p ≤ 0.05 (*), p ≤ 0.01 (**), p ≤ 0.001 (***), p ≤ 0.0001 (****). Each experiment comprises a minimum of 3 biological replicates. ***A)*** *Data taken from a 30-hour growth curve measuring fluorescence intensity and OD_{600} at regular intervals. Multiple t-tests were applied comparing the mean relative fluorescence between strains. The most statistically significant timepoint was further analyzed using Welch's unpaired t-test.* ***B)*** *Relative fluorescence of strains measured after 25 hours of growth.* ***C)*** *Relative fluorescence of strains measured after 25 hours of growth.*

Validating SabS interactions in *E. coli* using a two-plasmid reporter system

To further validate the interactions, the two-plasmid reporter system was tested in *E. coli* TOP10. This is consistent with previous studies, as the original two plasmid system (using pP_L and pXG10- based plasmids) was first established and used widely in *E.coli* (Urban & Vogel, 2007). Testing each interaction in *E. coli* allowed for cross-species comparisons, and assessment of consistency of the observed regulatory effects in AB5075. The pAMCK 2-plasmid system is compatible in both *E. coli* and *Acinetobacter*, and thus the same experimental set-up as described above was employed in *E. coli* strain TOP10 (Mogre et al., 2025).

In *E.coli*, SabS significantly repressed fluorescence intensity of ABUW_RS18870-sfGFP ($p < 0.01$) ,ABUW_RS00045-sfGFP ($p < 0.001$), and ABUW_RS13040 - sfGFP ($p < 0.01$) when compared with the control strain. SabS appears to repress fluorescence intensity of ABUW_RS15920 in comparison to the pAMCK15 carrying strain, however since n=2 in this dataset further experiments will be needed to assess significance (**Figures 1.7 and 1.8**). SabS repressed translation of ABUW_RS18870-sfGFP in both *Acinetobacter* and in *E. coli*, suggesting that SabS represses translation of ABUW_RS18870. However, while SabS enhanced fluorescence intensity of ABUW_RS00045-sfGFP in *Acinetobacter*, it significantly reduced it in *E. coli*. In addition, there was no significant effect of SabS on ABUW_RS13040-sfGFP fluorescence, however in *E.coli* fluorescence intensity was significantly lower in the pAMCK14-SabS expressing strain.

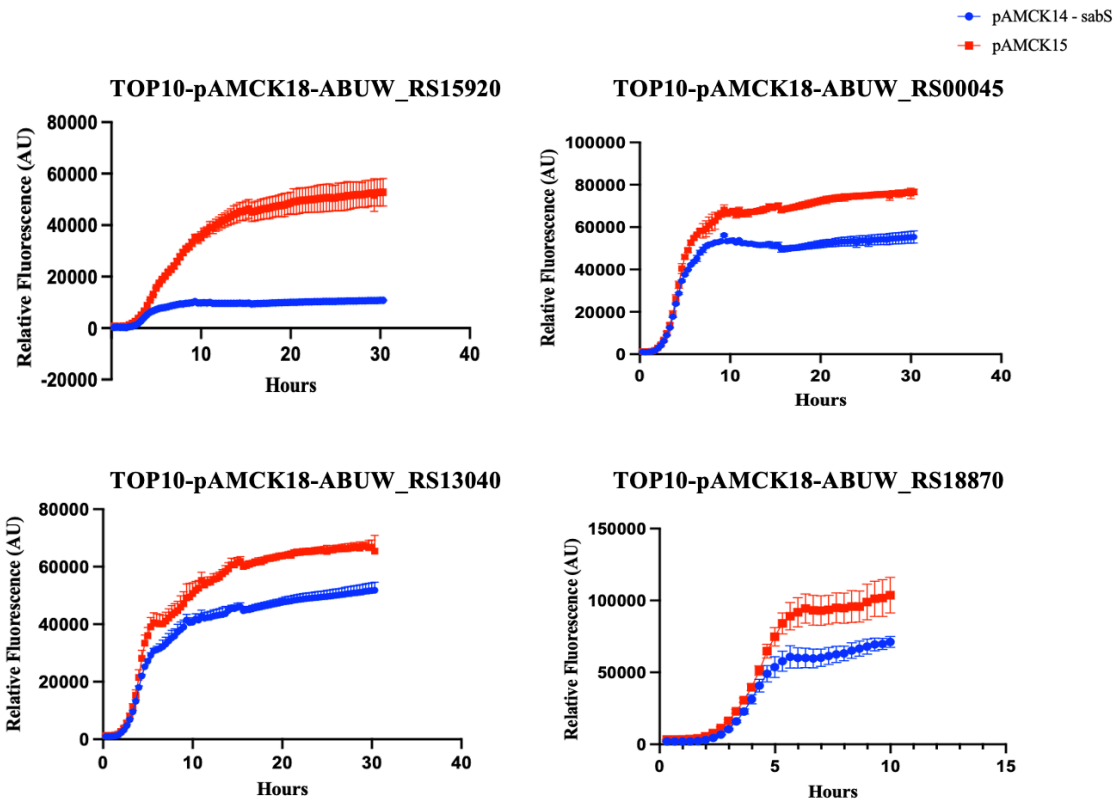

Figure 1.7: Relative fluorescence of TOP10 reporter strains.

E. coli TOP10 strains carrying pAMCK18 – target were co-expressed with either pAMCK14 – sabS or pAMCK15. Cultures were inoculated from a starting OD_{600} of 0.01 and grown for 30 hours in 96 well plates. Fluorescence and OD_{600} measurements were taken at regular intervals. Data is shown as mean ± SD with individual points for each biological replicate (n ≥ 3 per condition, n = 2 for ABUW_RS15920). Strains were compared using multiple t-tests with FDR correction.

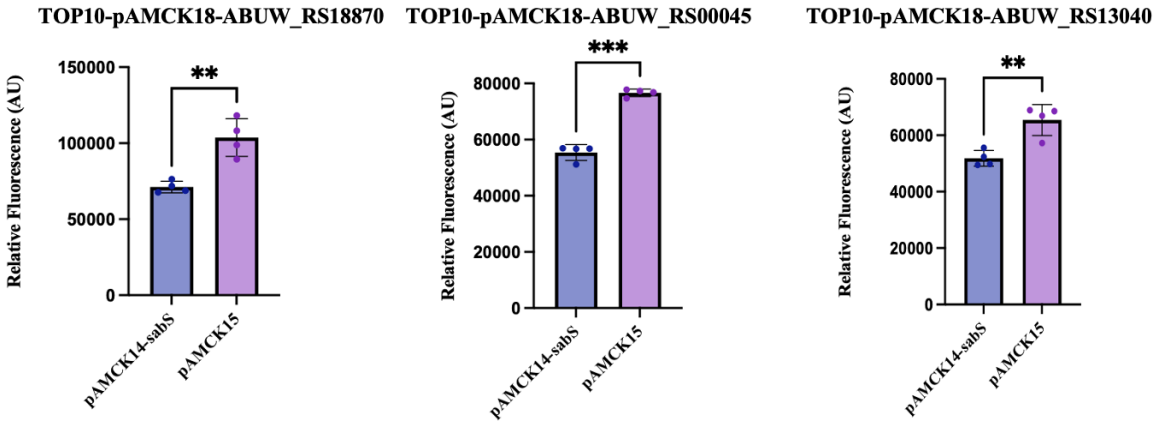

Figure 1.8 : Relative fluorescence of TOP10 reporter strains.

Data taken from a 30-hour growth curve measuring fluorescence intensity and OD_{600} at regular intervals. Multiple t-tests were applied comparing the mean relative fluorescence between strains. The most statistically significant timepoint was further analyzed using Welch's unpaired t-test. Significance thresholds are defined as follows; ns = not significant; $p \leq 0.05$ (*), $p \leq 0.01$ (**), $p \leq 0.001$ (***), $p \leq 0.0001$ (****).

Impact of *sabS* chromosomal deletion on translation of target mRNAs

To further investigate the impact of SabS *in vivo*, pAMCK18-target plasmids were expressed in AB5075 Δ*sabs* mutant strains. As a control, pAMCK18-target plasmids were also expressed in AB5075 wild-type strains. Strains were grown for 30 hours, and fluorescence intensity was measured at regular intervals throughout the time course.

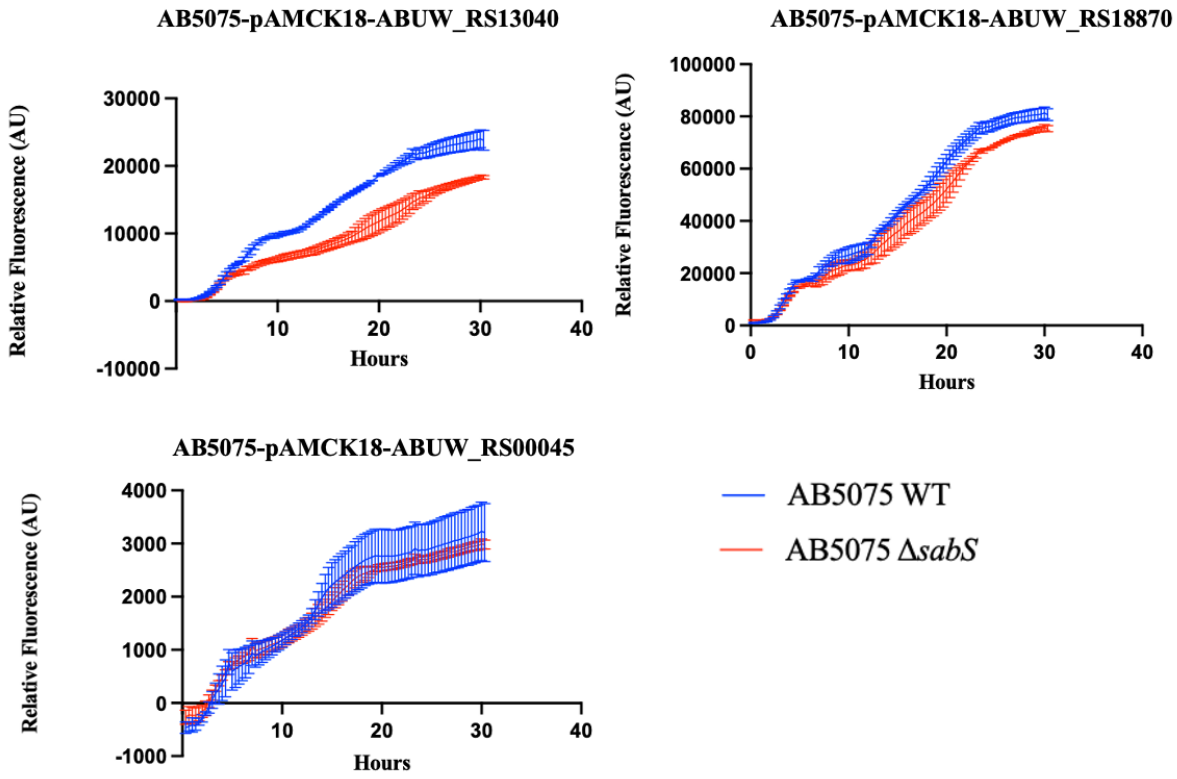

Figure 1.9: Relative fluorescence of pAMCK18-target strains in both WT AB5075 and Δ*sabs* measured over a period of 30 hours.

AB5075 ΔsabS mutant strains carrying pAMCK18-target plasmids were inoculated from a starting OD_{600} of 0.01 and grown for 30 hours in 96 well plates. Fluorescence and OD_{600} measurements were taken at regular intervals. Data is shown as mean ± SD with individual points for each biological replicate (n ≥ 3). Strains were compared using multiple t-tests with FDR correction.

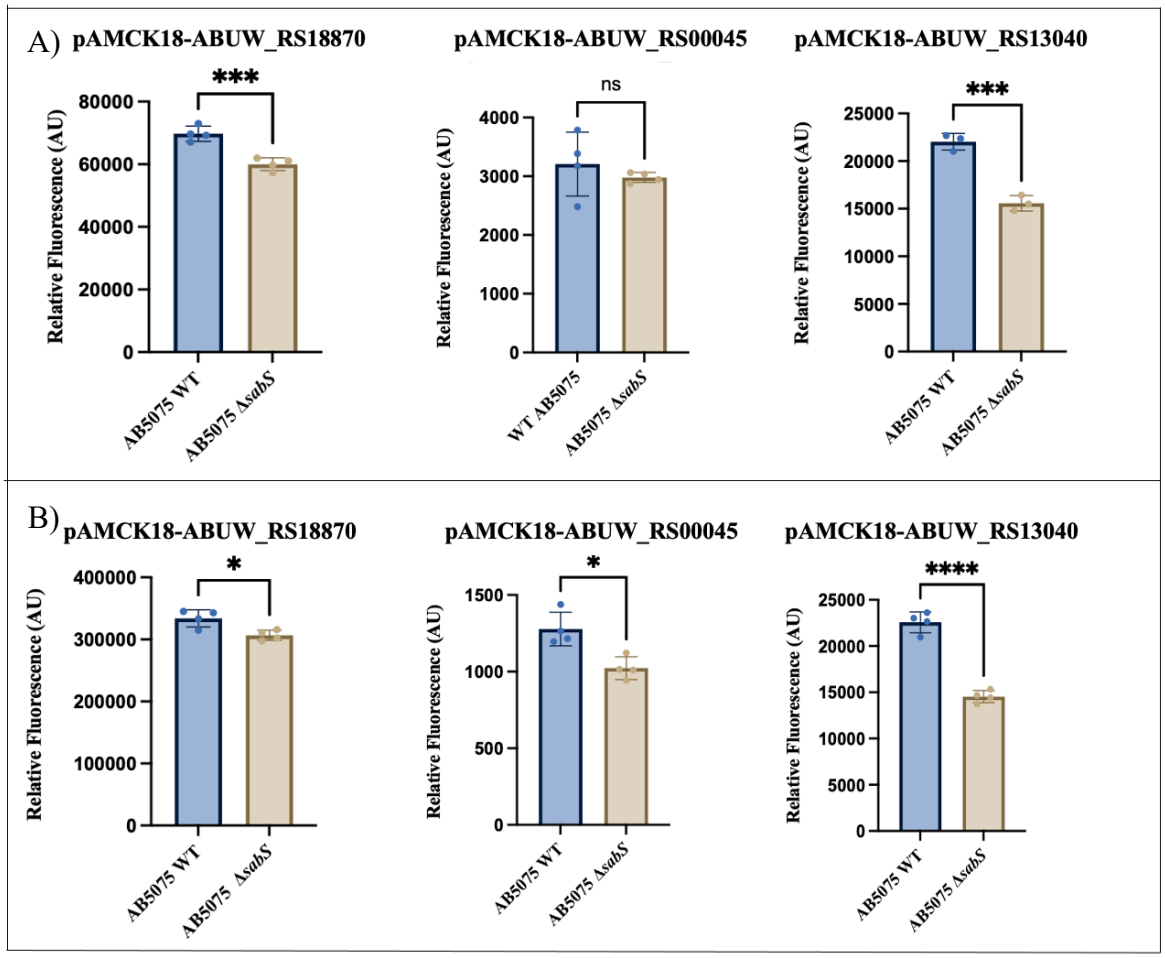

Figure 1.10: Effect of pAMCK18-target expression in wild-type AB5075 compared to AB5075 *ΔsabS*.

Data were analyzed using an unpaired Welch's t test comparing A. baumannii AB5075 WT and ΔsabS. ns = not significant; ns = not significant; p ≤ 0.05 (*), p ≤ 0.01 (**), p ≤ 0.001 (***), p ≤ 0.0001 (****). Each experiment comprises a minimum of 3 biological replicates. Data is shown as mean ± SD with individual points for each biological replicate (n ≥ 3 per condition). ***A)*** *Data taken from a 30-hour growth curve measuring fluorescence intensity and* OD_{600} *at regular intervals. Multiple t-tests were applied comparing the mean relative fluorescence between strains. The most statistically significant timepoint was further analyzed using Welch's unpaired t-test.* ***B)*** *Relative fluorescence of strains measured after 30 hours of growth.*

AB5075 *ΔsabS* - pAMCK18-ABUW_RS18870 showed lower fluorescence intensity at 21 hours when compared with the wild-type strain ($p < 0.001$). In addition , AB5075 Δ*sabS* - pAMCK18-ABUW_RS13040 showed lower fluorescence levels at 24 hours when compared with the wild-type strain ($p < 0.001$) (**Figure 1.9**, **Figure 1.10, A)**). Endpoint measurements at 30 hours of relative fluorescence also showed a reduction of fluorescence in Δ*sabS* mutant strains in comparison with wild-type, when carrying pAMCK18-ABUW_RS18870 and pAMCK18-ABUW_RS13040 (**Figure 1.9**, **Figure 1.10, B)**), indicating upregulation of these mRNAs by SabS. There was no significant difference in fluorescence between AB5075 pAMCK18-ABUW_RS00045 wild-type and Δ*sabS* mutant strains when analyzed from kinetic measurements, however endpoint measurements showed a decrease in fluorescence intensity in the Δ*sabS* mutant strain when compared with wild-type, indicating upregulation of ABUW_RS00045 by SabS.

Impact of *sigAB* chromosomal deletion on translation of target mRNAs

Recent experiments have shown that the ECF sigma factor SigAB directly regulates SabS (Bacon et al., 2025). Furthermore, it has been shown that SabS mediates SigAB dependent metal resistance in *A. baumannii* ATCC 19606 (Bacon et al., 2025). In addition, overexpression of SigAB results in downregulation of genes that are direct targets of Sabs (Bacon et al., 2025). As a result, it has been hypothesised that SabS is either directly or indirectly modulating SigAB-dependent metal resistance (Bacon et al., 2025). However, the exact mechanisms of SigAB mediated regulation of SabS are unknown (Bacon et al., 2025). Hence, it was critical to analyze the effects of target mRNA expression in a Δ*sigAB* strain. To analyze the extent to which SigAB regulates SabS in vivo, two SabS targets were cloned in pAMCK18 and expressed in both AB5075 Δ*sigAB* and AB5075 WT.

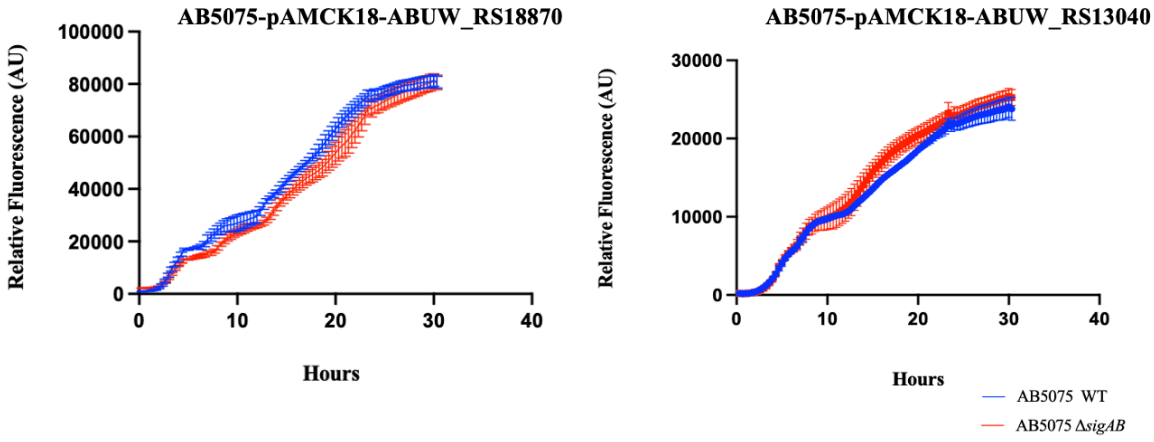

Figure 1.11: Relative fluorescence of pAMCK18-target strains in both WT AB5075 and Δ*sigAB* measured over a period of 30 hours.

AB5075 ΔsigAB mutant strains carrying pAMCK18-target plasmids were inoculated from a starting OD_{600} of 0.01 and grown for 30 hours in 96 well plates. Fluorescence and OD_{600} measurements were taken at regular intervals. Data is shown as mean ± SD with individual points for each biological replicate (n ≥ 3). Strains were compared using multiple t-tests with FDR correction.

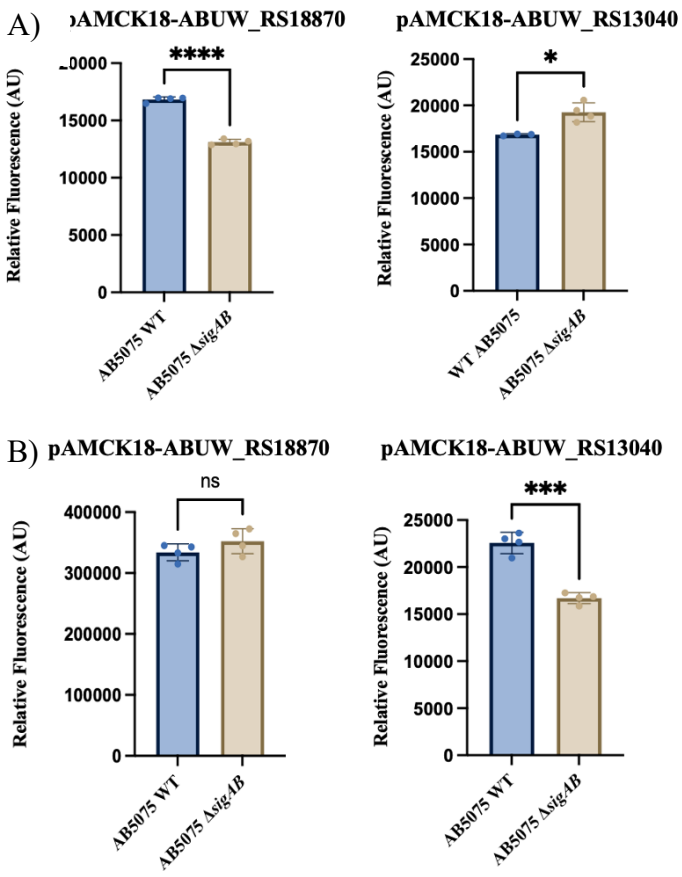

Figure 1.12: Effect of pAMCK18-target expression in wild-type AB5075 compared to AB5075 *ΔsigAB*.

Data were analyzed using an unpaired Welch's t test comparing A. baumannii AB5075 WT and ΔsigAB. ns = not significant; p ≤ 0.05 (*), p ≤ 0.01 (**), p ≤ 0.001 (***), p ≤ 0.0001 (****). Each experiment comprises a minimum of 3 biological replicates. Data is shown as mean ± SD with individual points for each biological replicate (n ≥ 3 per condition). ***A)*** *Data taken from a 30-hour growth curve measuring fluorescence intensity and OD_{600} at regular intervals. Multiple t-tests were applied comparing the mean relative fluorescence between strains. The most statistically significant timepoint was further analyzed using Welch's unpaired t-test.* ***B)*** *Relative fluorescence of strains measured after 30 hours of growth.*

Expression of ABUW_RS18870 from pAMCK18 was significantly lower in AB5075 Δ*sigAB* at hour 5 when compared with the wild-type strain (p = < 0.001). Conversely, expression of ABUW_RS13040 was significantly higher in Δ*sigAB* at hour 18 when compared with the wild-type strain (p = < 0.05) (**Figure 1.11**, **Figure 1.12, A)**). This would indicate that SigAB may be involved in repression of ABUW_RS13040 translation and may enhance translation of ABUW_RS18870. Endpoint measurements did not align with kinetic analysis and showed an increase in fluorescence in wild-type AB5075 carrying pAMCK18-ABUW_RS13040 compared with AB5075 Δ*sigAB,* while there was no significant difference comparing AB5075 Δ*sigAB* and wild-type strains carrying pAMCK18- ABUW_RS18870 (**Figure 1.12, B)**). Overall, results from the two plasmid reporter systems varied depending on the host. SabS appeared to downregulate ABUW_RS18870 in both *E.coli* and *A. baumannii*, however appeared to up-regulate it in a deletion background. Fluorescence was higher in wild-type AB5075 when compared with a Δ*sabS* mutant strain, indicating that SabS upregulates translation of ABUW_RS18870 in a native background. SabS increased the fluorescence intensity of ABUW_RS00045 - sfGFP in *A. baumannii* and reduced it in *E. coli*. In addition, ABUW_RS00045-sfGFP also showed higher fluorescence intensity in wild-type AB5075 when compared with a Δ*sabS* mutant strain, indicating upregulation of ABUW_RS00045 by SabS in *A. baumannii.* SabS did not influence fluorescence intensity of ABUW_RS13040-sfGFP in *Acinetobacter* and reduced it in *E. coli*. ABUW_RS13040-sfGFP showed higher fluorescence intensity in a wild-type AB5075 strain when compared with a Δ*sabS* mutant strain.

Growth phenotypes of Δ*sabS* and Δ*sigAB* mutants under environmental stress conditions

Alternative sigma factors have long been implicated in the regulation of stress responses in bacteria, they are promoter specific and can direct RNAP to specific promoter sites, and thus initiate transcription of specific genes. They are involved in stress responses ranging from iron uptake, cell wall maintenance and motility (Woods & McBride, 2017). SigAB has been associated with cell envelope and copper stress in *A. baumannii*. Furthermore, knockdowns of *sigAB* and *sabS* have resulted in similar phenotypes in *A. baumannii* (Bacon et al., 2025). As such, the effects of *sigAB* and *sabS* deletions were studied under various stress conditions.

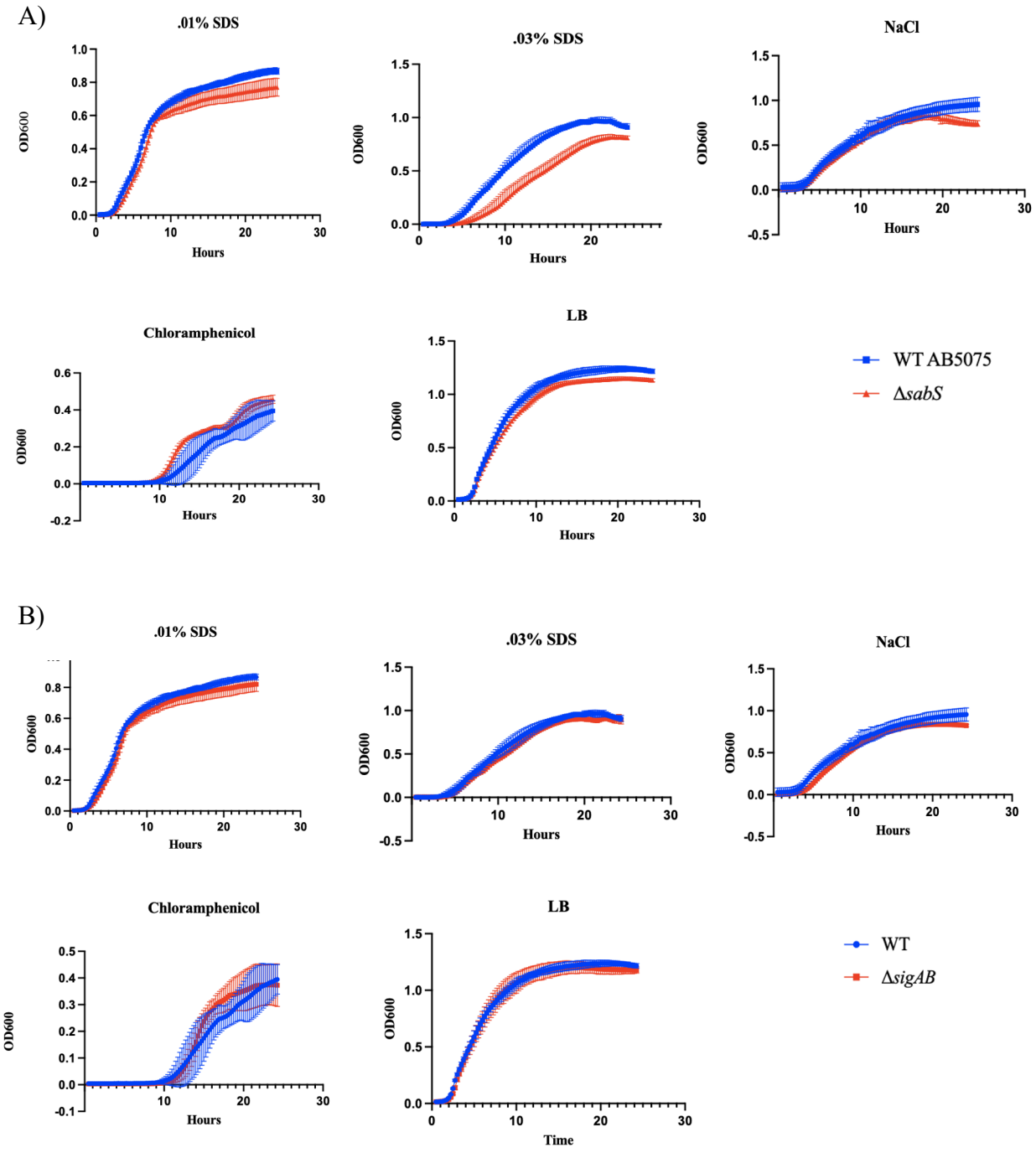

Figure 1.13: Growth of AB5075 wild-type, AB5075 *ΔsabS,* and AB5075 *ΔsigAB* under different stress conditions.

A) *AB5075 wild-type (blue), AB5075 ΔsabS (red)* ***B)*** *AB5075 wild-type (blue) and AB5075 ΔsigAB (red).*

Impact of *sabS* and *sigAB* deletions on the envelope stress response

The cell envelope of Gram-negative bacteria comprises the inner membrane, periplasm, and peptidoglycan, and acts to protect the cell from its surroundings. Various environmental stressors can induce envelope stress responses, which activate sensor proteins and initiates a signaling cascade, regulating gene expression in order to respond to cell damage (Mitchell & Silhavy, 2019). *A. baumannii* relies on the BfmRS two-component system to respond to outer membrane lipoprotein stress (Marotta et al., 2025). SigAB has shown to regulate copper stress in *A. baumannii*, and further has shown to have direct control of stringent response factor RelA. (Bacon et al., 2025) To investigate the role of SigAB and SabS during envelope stress , two concentrations of sodium dodecyl sulfate (SDS) were added to the growth media to induce membrane stress (0.01% and 0.03%). SDS is a well-established bacterial cell membrane stressor, and as such was chosen to investigate the effects of membrane stress in AB5075 Δ*sigAB* strains. (Zhu et al., 2024). Since SabS is included in the SigAB regulon, effects of SDS on growth were also tested in Δ*sabS* strains (Bacon et al., 2025). AB5075 *Δsabs* showed impaired growth compared to wild-type AB5075 when grown in both 0.01% and 0.03% SDS media, however this difference was not seen in AB5075 Δ*sigAB* when compared to the wild-type strain (**Figure 1.13, A),B)**).This suggests that SabS has a role in mediating envelope stress in AB5075, however given that the same growth phenotype was not observed in the Δ*sigAB* mutant, that this function of SabS is not mediated by SigAB.

Impact of *sabS* and *sigAB* deletions on the osmotic stress response

Bacterial sigma factors such as RpoS in *E. coli* regulate osmotic stress responses. (Liao et al., 2020) To investigate the effects of osmotic stress in *sigAB* and *sabS* deletion strains, they were grown for a period of 24 hours in L-Broth supplemented with 500mM NaCl. There was no difference between AUC means for either AB5075 *ΔsabS* or AB5075 *ΔsigAB* when compared

to AB5075 wild-type, indicating that SabS and SigAB are not essential in mediating the osmotic stress response in AB5075 **(Figure 1.13)**.

Impact of *sabS* and *sigAB* deletions on the antibiotic stress response

In addition, ECF sigma factors have been shown to influence antibiotic stress responses. (Woods & McBride, 2017) In this instance, chloramphenicol was used to assess the effect of *sigAB* and *sabS* deletions under antibiotic stress. Chloramphenicol is a broad-spectrum antibiotic that prevents protein synthesis by binding to the 50S subunit of the bacterial 70S ribosome. (Moffa & Brook, 2015) Both AB5075 Δ*sigAB* and Δ*sabS* strains were grown in L-broth supplemented with the sub-inhibitory concentration of 50ug/mL of chloramphenicol. There was no significant difference between AUC means for either AB5075 *ΔsabS* or AB5075 *ΔsigAB* when compared to AB5075 wild-type **(Figure 1.14)**. In this instance, it could suggest that SabS and SigAB are not essential for mediating tolerance to inhibition of protein translation.

Antibiotic susceptibility tests

A. baumannii can develop resistance to β-lactam antibiotics, including carbapenems which are typically used as a last-line treatment against MDR bacteria in hospital settings (Černiauskienė et al., 2023). *A. baumannii* mediates resistance to β-lactamases through enzyme mediated inactivation of the target (β-lactamases production), modulation of efflux pump activity, decreasing membrane permeability, and alteration of penicillin-binding proteins (Kyriakidis et al., 2021). Small RNAs are often involved in regulating antibiotic resistance mechanisms in Gram-negative bacteria, including *A. baumannii*. In addition, carbapenem resistance in *A. baumannii* has been linked to sRNA regulation (Mediati et al., 2021). Therefore, the effect of three different classes of β-lactam antibiotics were tested on AB5075 Δ*sabS,* AB5075 Δ*sigAB*. Carbapenems (imipenem, meropenem), cephalosporins, (cefepime, ceftazidime), and penicillins (piperacillin, ticarcillin) were tested. No difference in zone of inhibition across

strains was observed when compared to AB5075 wild-type. Hence, the chromosomal deletion of *sabS* and *sigAB* did not significantly alter the susceptibility of AB5075 to any of the antibiotics. The mean zone of inhibition from three independent biological replicates for each strain is outlined in **Table 1.12.**

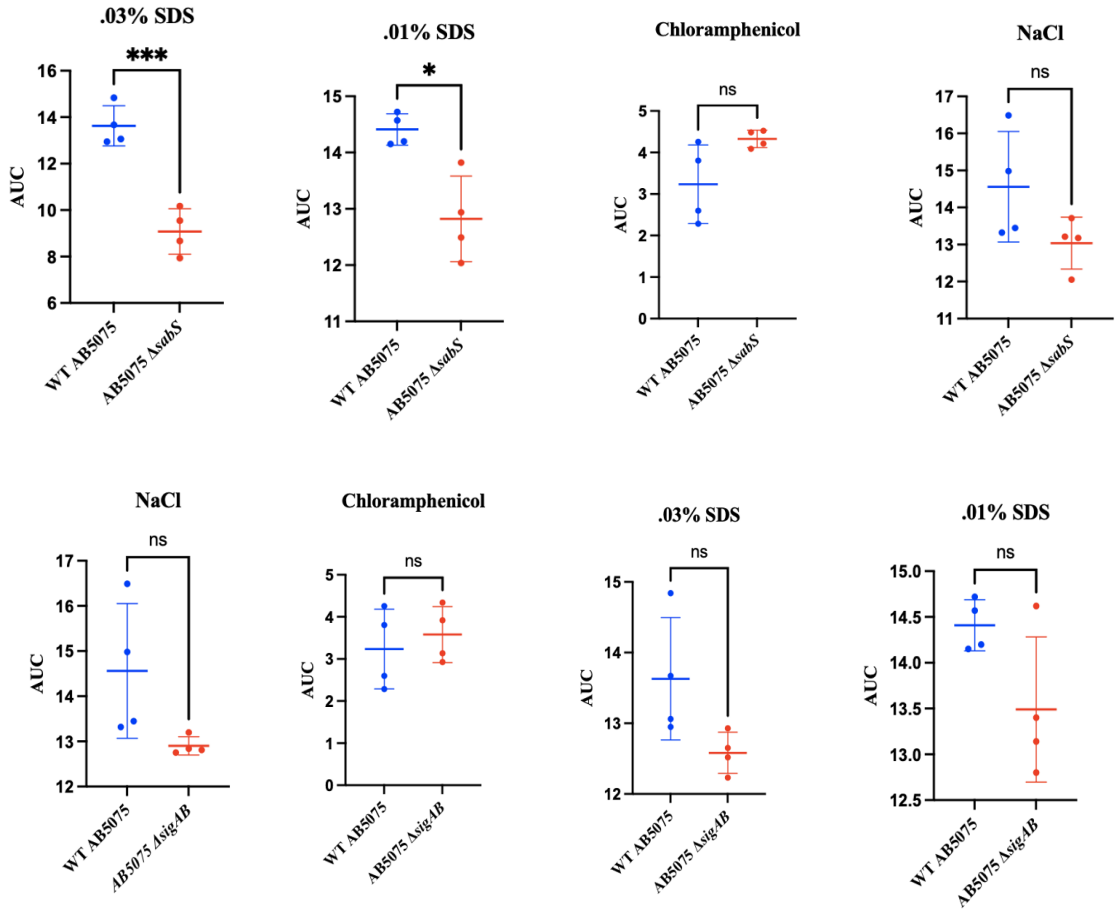

Figure 1.14: Growth experiments - bar graphs of Area under the curve (AUC) means for each biological replicate.

Area under the curve was calculated for each biological replicate over the 24-hour growth period. Statistical analysis was carried out using unpaired t-test between mean AUC for each strain.

Table 1.12: Mean zone of inhibition diameters (cm) of AB5075 wild-type, AB5075 Δ*sabS*, *and* AB5075 Δ*sigAB*. ("R" is used to denote resistant strains which had no observable sensitivity to the antibiotic)

	Zone of inhibition (cm)		
Antibiotic	AB5075 wild-type	AB5075 Δ*sabS*	AB5075 Δ*sigAB*
Meropenem	R	R	R
Cefepime	R	R	R
Ceftazidime	R	R	R
Piperacillin/Tazobactam	R	R	R
Imipenem	1.2	1.2	1.2
Ticarcillin	R	R	R

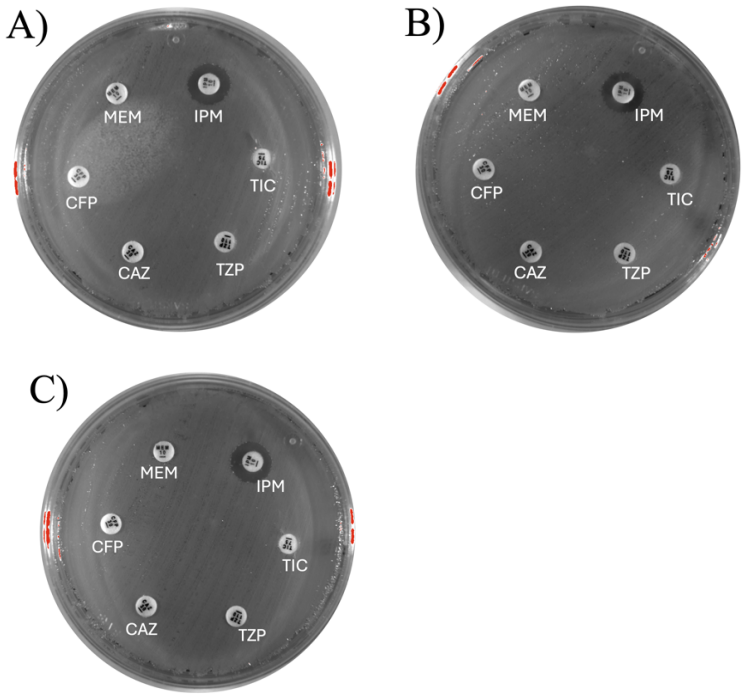

Figure 1.15: Antibiotic susceptibility test of AB5075 strains. A) AB5075 Wild-Type. B) AB5075 Δ*sabS*, C) AB5075 Δ*sigAB*.

Antibiotics are denoted as follows; MEM= meropenem (10 µg), IPM = Imipenem (10µg), TIC = Ticarcillin (75µg), TZP = Piperacillin/Tazobactam (110µg), CAZ = Ceftazidime (30µg), CFP = Cefepime (30µg).

Summary:

- SabS was identified as a potential 'keystone' sRNA with four candidate mRNA targets.
- In *A. baumannii* AB5075:
  - SabS represses ABUW_RS18870 translation.
  - SabS enhances ABUW_RS00045 translation.
  - SabS does not significantly affect translation of ABUW_RS13040.
- In *E.coli* TOP10, SabS reduces fluorescence intensity of all targets (ABUW_RS15920, ABUW_RS00045, ABUW_RS13040, ABUW_RS18870).
- In *A. baumannii* AB5075 Δ*sabS:*
  - SabS increases translation of ABUW_RS18870-sfGFP and ABUW_RS13040-sfGFP.
  - SabS did not influence fluorescence intensity of ABUW_RS00045-sfGFP in kinetic timepoint measurements and downregulates the target in endpoint measurements.
  - In *A. baumannii* AB5075 Δ*sigAB:*
    - SigAB represses ABUW_RS13040-sfGFP in a single-timepoint measurement but upregulates in kinetic measurements.
    - SigAB increases fluorescence intensity of ABUW_RS18870-sfGFP in a single-timepoint measurement yet showed no significant difference in kinetic measurements.
  - Under envelope stress (SDS, 0.01% and 0.03%): AB5075 *ΔsabS* showed impaired growth and AB5075 *ΔsigAB* showed no significant difference compared to WT AB5075.
  - Neither AB5075 *ΔsabS* or AB5075 *ΔsigAB* strains showed significant growth differences compared to AB5075 WT under osmotic or antibiotic stress.

Chapter 2: Hi-GRIL-seq

The development of high-throughput sequencing methods has significantly aided in the discovery of novel sRNA-mRNA interactions. Early methods involved the crosslinking of sRNAs to their associated RBPs and subsequent immunoprecipitation and sequencing (Georg et al., 2020).

The development of Hi-GRIL-seq (high throughput global sRNA target identification by ligation and sequencing) was developed to allow for characterisation of mRNA-sRNA interaction pairs without relying on previous knowledge of RBPs. Hi-GRIL-seq involves inducing expression of T4 RNA ligase *in vivo*, followed by high throughput sequencing (Zhang et al., 2017) (**Figure 2.1**). This method has aided in the discovery of novel sRNA-mRNA pairs and has uncovered the role of sRNA Aar as a translational repressor of virulence associated outer membrane protein CarO (Hamrock et al., 2024). The original Hi-GRIL-seq experiment involved the growth of AB5075 expressing T4 RNA ligase to early stationary phase (~ OD_{600} 2.0) before induction with L-arabinose (Hamrock, 2025). To expand on these results and assess potential differences in sRNA expression across growth phases, this experiment was carried out at early exponential phase (EEP) and late stationary phase (LSP) before induction. Growth phase-dependent sRNA expression has been documented in some bacterial species, with many sRNAs exhibiting differential expression during stationary phase as bacteria activate stress response pathways (Raad et al., 2021). In particular, LSP was chosen as a growth phase due to many stress response sRNAs exhibiting differential expression in stationary phase (Raad et al., 2021).

In this experiment, RNA was isolated from *A. baumannii* AB5075 PVRL2Z - *t4rnlI* cells at both EEP (OD_{600} 0.1) and LSP (OD_{600} 4.0) in two separate experiments. Each experiment was carried out with four biological replicates. Prior to RNA isolation, cells were incubated for one hour with 100mM of L-arabinose to induce T4 RNA ligase expression. As a control, cells were grown for one hour without the addition of L-arabinose.

100mM L-arabinose is sufficient for T4 RNA ligase induction.

In this experiment, the T4 RNA Ligase encoding gene *(t4rnlI*) was placed under control of the arabinose inducible pBAD promoter on the pVRL2Z plasmid. Expression of T4 RNA ligase causes ligation of sRNA molecules to interacting RNAs. Since RNA-RNA pair accumulation is lethal to the bacterial cell, experiments were previously carried out to determine optimal concentration of L-arabinose needed for induction without causing excessive cell death (Hamrock, 2025). This involved measuring the optical density of *A. baumannii* cultures grown with varying concentrations of L-arabinose. Prior to carrying out this experiment, the effect of 100mM L-arabinose was re-tested to ensure functionality of the T4 RNA ligase gene. This involved growing AB5075 pVRL2Z-*t4rnlI* to the desired optical density and adding 100mM of L-arabinose. As a control, 3 biological samples were left un-treated. The samples were then incubated for one hour. Calculation of CFU/mL count per culture showed that 100mM of L-arabinose is sufficient to allow RNA-RNA ligation without causing excessive cell death **(Figure 2.2)**.

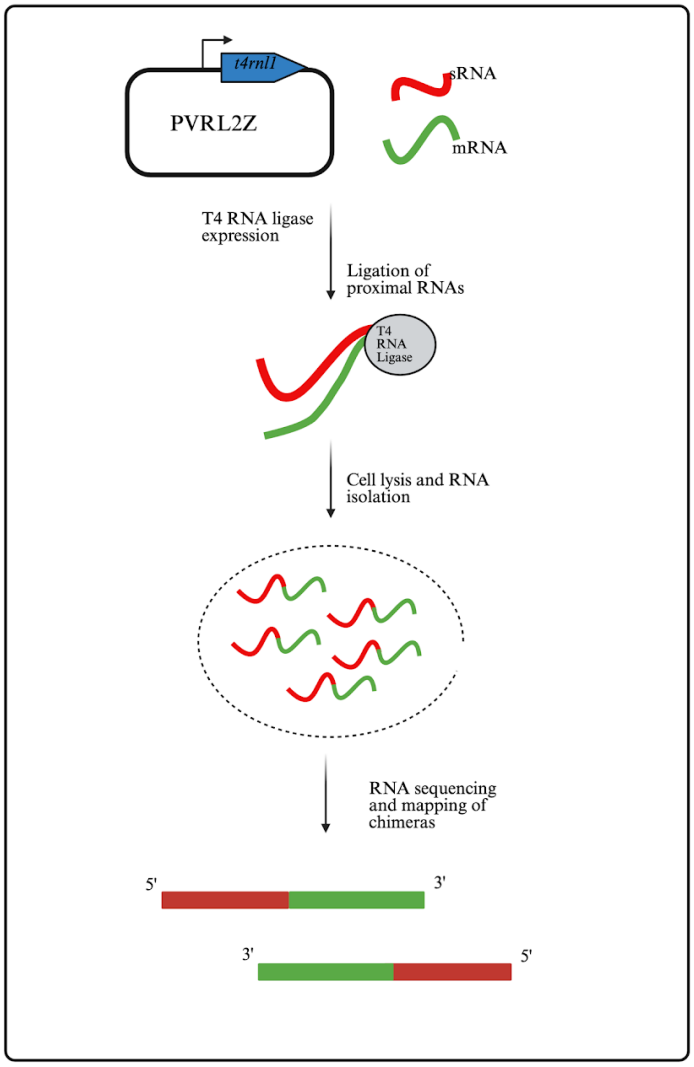

Figure 2.1: Schematic of Hi-GRIL-seq experimental setup

A. baumannii AB5075 pVRL2Z - t4rnlI cells were grown to EEP (OD_{600} 0.1) and LSP (OD_{600} 4). Expression of T4 RNA ligase was induced by addition of 100mM of L-arabinose. Cells were lysed and total RNA was isolated and sequenced. Chimeras were mapped to the A. baumannii AB5075 genome and analyzed for putative mRNA-sRNA interactions.

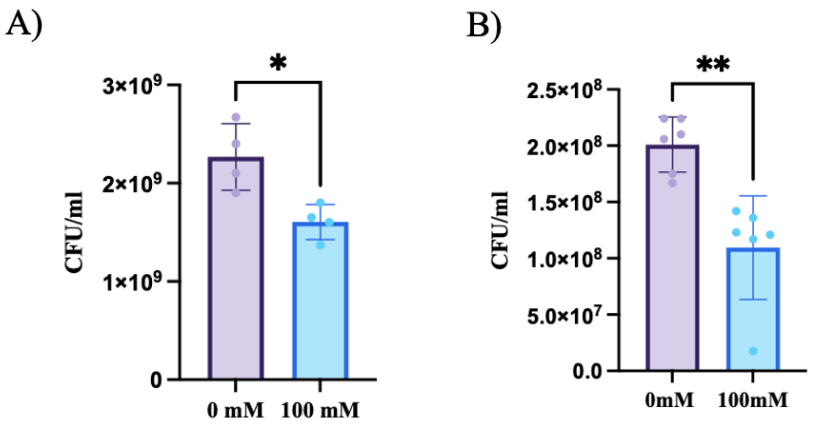

Figure 2.2: 100mM L-arabinose is sufficient for T4 RNA ligase induction without causing excessive cell death.

Colony forming units (CFU/ml) of AB5075 pVRL2Z-t4rnlI after one hour incubation with either 0mM or 100mM L-arabinose. Cells were grown to ~ OD_{600} 4 ***(A)*** *and* OD_{600} *~ 0.1* ***(B)****, before induction. Error bars represent the standard deviation between four biological replicates. Statistical analysis carried out using an unpaired t-test. (ns = not significant; $p \leq 0.05$ (*), $p \leq 0.01$ (**), $p \leq 0.001$ (***), $p \leq 0.0001$ (****).*

Hi-GRIL-seq at Late Stationary Phase (LSP)

Cultures of AB5075 PVRL2Z - *t4rnlI* were grown to ~ OD_{600} 4, before a one-hour induction with either 0mM (non-induced) or 100mM (induced) of L-arabinose. Total RNA was isolated from two samples of both induced and non-induced cultures and used to construct cDNA libraries for RNA sequencing. Hi-GRIL-seq from OD_{600} 4 did not yield detectable chimeras.

Hi-GRIL-seq at Early Exponential Phase (EEP)

Cultures of AB5075 PVRL2Z -*t4rnlI* were grown to ~ OD_{600} 0.1, before one hour induction with either 0mM (non-induced) or 100mM (induced) of l-arabinose. Total RNA was isolated from two samples of both induced and non-induced cultures and used to construct cDNA

libraries for RNA sequencing. The experiment was carried out using biological duplicates for induced and non-induced samples and sent for sequencing.

Analysis of Hi-GRIL-seq derived RNA-RNA chimeras

Sequencing results showed an enrichment of chimeras in the induced samples, indicating functionality of the T4 RNA ligase gene. There were 2,374 chimeric reads across induced samples, and 474 chimeric reads across non-induced samples (~83% of chimeric reads came from induced samples). Several chimeras were found in non-induced samples, which could indicate basal expression of T4 RNA ligase, which could overrepresent proximal RNAs that are not functionally related. Chimeras were filtered to exclude those with >10% of reads derived from the non-induced samples **(Figure 2.3)**. To ensure all interactions were true, trans-RNA interactions, chimeras where the ligation site was within 500 nucleotides of the sRNA locus were filtered, excluding self-ligated molecules. Post-filtering, there were 450 sRNA containing reads across induced samples, and 10 across non-induced samples. Of these, there were 10 distinct sRNA containing chimeras across induced samples, and 3 across non-induced samples. SabS was found in two sRNA-mRNA pairs within the Hi-GRIL-seq dataset. The two interaction pairs were ABUW_RS03195, an OmpA family protein, and ABUW_RS00045, a hypothetical protein of unknown function **(Figure 2.4)**. The interaction between SabS and ABUW_RS00045 has been previously validated using a two-plasmid reporter system during this study, and therefore the remaining chimeras in the HI-GRIL- seq dataset may be treated as putative interactions for further investigation. In addition, 8 other high confidence putative sRNA-mRNA interactions were identified after filtering (≥10 ligation events) Notably, ABUW_RS03195 was found in chimeras with two other sRNAs, sRNA84, and sRNA24. sRNA97 was found to interact with three mRNAs, ABUW_RS13350 (CsrA, a carbon storage regulator), ABUW_RS14070 (a capsule assembly Wzi family protein) and ABUW_RS11140 (a hypothetical protein). The CsrA (Carbon Storage Regulator A) mRNA transcript was found in several sRNA containing chimeras with sRNA97 (CsrB). This was the most abundant interaction in the dataset, accounting for 257 chimeric reads across both induced conditions. A full list of sRNA containing chimeras with ≥10 sequencing reads is shown in **Table 2.1.**

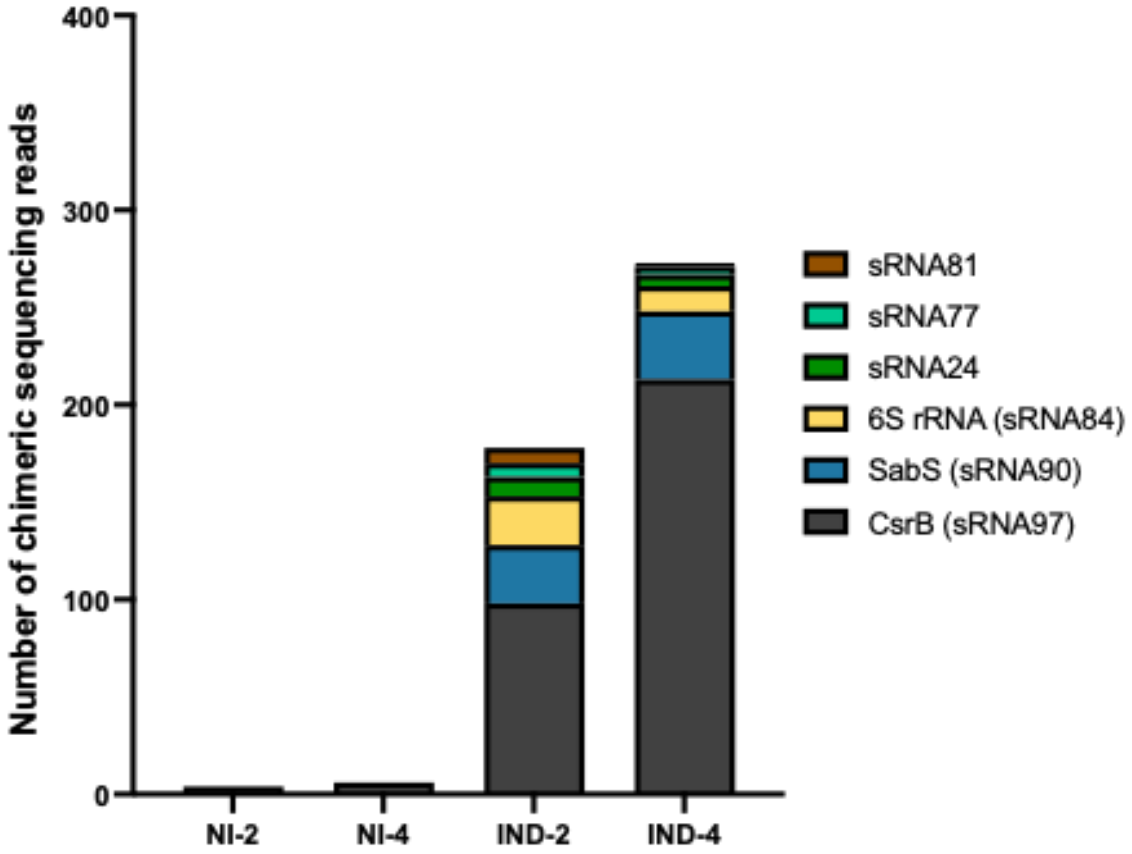

Figure 2.3: Graph of filtered chimeric sequencing reads by sRNA for each condition (≥10 sequencing reads).

Bar graph shows chimeras where less than 10% of sequencing reads are derived from the non-induced (NI) conditions, with no autoligation (500 nucleotides away from sRNA). Results from independent biological duplicates of each treatment are visualized as adjacent bars.

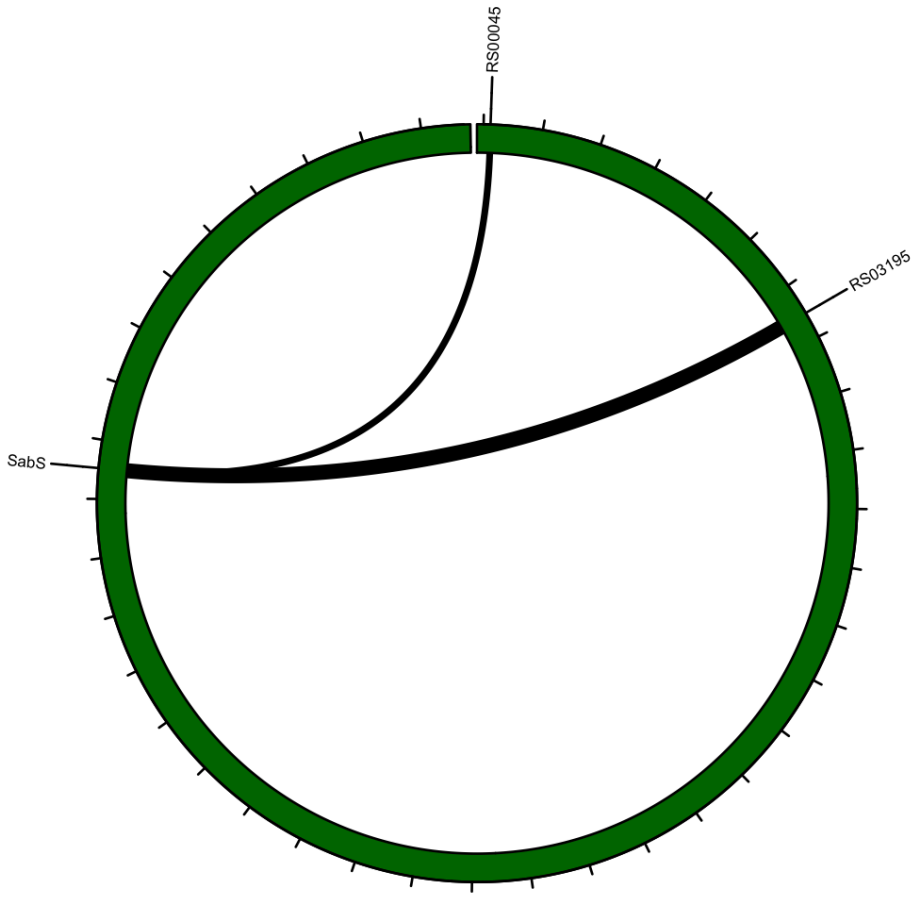

Figure 2.4: Hi-GRIL-seq data shows SabS is ligated with two mRNA targets.

Filtered chimeric reads show SabS is ligated to two putative mRNA targets. The circle represents the AB5075 chromosome, with line width corresponding to the number of chimeric sequencing reads.

Table 2.1: Hi-GRIL-seq reads with ≥10 sequencing reads, <10% sequencing reads from the NI conditions and no autoligation (500 nts away from sRNA)

sRNA	Gene	Function	NI-2	NI-4	IND-2	IND-4
SabS	ABUW_RS03195	OmpA family protein	0	0	23	22
SabS	ABUW_RS00045	hypothetical protein	0	0	7	13
sRNA24	ABUW_RS03195	OmpA family protein	0	0	10	6
sRNA81	ABUW_RS00825	putative porin	0	0	8	2
sRNA77	ABUW_RS16970	ABC transporter	0	0	7	4
sRNA84	ABUW_RS03195	OmpA family protein	0	0	22	5
sRNA84	ABUW_RS07500	hypothetical protein	0	0	3	8
sRNA97	ABUW_RS13350	carbon storage regulator CsrA	3	5	78	179
sRNA97	ABUW_RS14070	capsule assembly Wzi family protein	1	0	13	24
sRNA97	ABUW_RS11140	hypothetical protein	0	1	7	10

.

Summary:

- 100mM L-arabinose is sufficient for induction of T4 RNA ligase without causing excessive cell death.
- No detectable RNA-RNA chimeras were identified at LSP.
- 2,374 chimeric reads were identified in induced samples at EEP , with 474 identified in non-induced samples.
- SabS was found in two mRNA – sRNA interaction pairs:
    - ABUW_RS03195 (OmpA family protein)
    - ABUW_RS00045 (hypothetical protein)
  - Abundant interactions:
    - ABUW_RS03195 with sRNA24, sRNA84 and sRNA84.
    - sRNA97 with ABUW_RS13350 (CsrA)
    - ABUW_RS14070 (Wzi family protein)
    - ABUW_RS11140 (hypothetical protein)
  - sRNA97-CsrA was the most abundant interaction in the dataset, accounting for 257 reads across induced samples.

Discussion

Characterization of small RNA mediated gene regulation in *A. baumannii* is still in its infancy, however accumulating research points toward post-transcriptional regulation as a mechanism by which bacteria fine tune stress responses. sRNAs are encoded from independent transcripts or processed from mRNAs. (Mediati et al., 2021). Mechanisms of *trans*- encoded sRNA mediated regulation of mRNAs is multifaceted and includes inhibition of translation by sequestration of the ribosome binding site (RBS), as well as promoting RNase E mediated degradation of the mRNA transcript. Conversely, sRNAs can enhance translation by stabilizing the mRNA transcript, as well as disrupting secondary structures to allow ribosomes to access the RBS. sRNAs have been shown to rapidly respond to stress responses, have shown to act on existing mRNAs and modulate either translation or degradation in response to stress. Importantly, small RNAs modulate responses involved in antibiotic susceptibility, and have shown to post-transcriptionally regulate porin proteins, thus regulating antibiotic uptake. In addition, sRNAs regulate LPS biosynthesis at the post-transcriptional level, maintaining structure of the OM in Gram-negative bacteria, as well as regulate biofilm formation. As such, this positions small RNAs as potential therapeutic targets against MDR pathogens (Yang et al., 2025a).

Investigations into the functions of uncharacterized sRNA-mRNA interactions is critical to understand the AMR mechanisms of MDR pathogens such as *A. baumannii.* In this study, we sought to characterize the role of small RNA SabS, as it has been overrepresented in a HI-GRIL-seq dataset (Hamrock, 2025). SabS had been previously proposed as a potential ‘keystone’ sRNA, simultaneously regulating multiple targets within *A. baumannii* AB5075. Keystone sRNAs often form regulatory hubs, and as such could play important roles in stress and AMR responses within the cell. For example, the small RNA PhrS in *Pseudomonas aeruginosa* , which regulates approximately 800 mRNAs, and GcvB in *E. coli*, shown to bind to over 150 targets (Gebhardt et al., 2023).

Interactions between SabS and four mRNAs encoding hypothetical proteins were tested in this study. The newly developed pAMCK two plasmid fluorescent reporter system was employed to verify these interactions in both *A. baumannii* AB5075, and *E. coli* TOP10 (Mogre et al., 2025).

Two plasmid reporter results of SabS-target mRNA interactions in differed in *A. baumannii* and *E. coli*, suggesting that species specific effects may cause these differences. Experiments in *A. baumannii* were carried out in wild-type strains, which contains a chromosomal copy of SabS. A *sabS* mutant was available; however, this strain still carried the apramycin resistance gene typically used for selection of the pAMCK14 reporter plasmid, and as a result is incompatible with the pAMCK 2-plasmid system. Expression of SabS significantly reduced the fluorescence intensity of pAMCK18-ABUW_RS18870 carrying strains in both *A. baumannii* and *E. coli*, indicating a negative regulatory effect of Sabs on ABUW_RS18870. However, in a SabS deletion AB5075, ABUW_RS18870-sfGFP showed higher expression in a wild-type AB5075 strain compared with the AB5075 Δ*sabS* mutant strain, which would suggest that SabS stabilizes ABUW_RS18870-sfGFP mRNA. This could suggest that ABUW_RS18870 is regulated by other sRNAs in addition to SabS. The effect of Sabs was contradictory for *E. coli* and *A. baumannii* strains carrying pAMCK18-ABUW_RS00045, as SabS appeared to enhance translation of this mRNA in *A. baumannii*, yet in *E. coli* the opposite effect was observed. In the SabS deletion background, a lower level of fluorescence was observed of ABUW_RS00045 when compared with the wild-type strain, consistent with *A. baumannii* two-plasmid reporter results. Results were consistent with a role of activating translation of ABUW_RS00045 within *A. baumannii*, however it is unclear why the opposite effect was observed in *E. coli.* One possible explanation for this is that the RBP Hfq in *A. baumannii* has a larger C-terminal domain, which influences sRNA-mRNA binding outcomes, and could be causing strain specific differences in sRNA-mRNA binding (A. Sharma et al., 2018). Further experiments could explore the effect of *A. baumannii* Hfq in *E.coli*, as this may be the cause of strain specific differences. For both ABUW_RS18870 and ABUW-RS00045, it would be important to quantify protein levels from chromosomal genes, to rule out effects caused using heterologous plasmids and to understand the role of SabS at a physiological level. SabS did not appear to have any significant regulatory effects on the expression of ABUW_RS13040 in *A. baumannii*, however showed a significant reduction of fluorescence intensity upon SabS overexpression in

E. coli TOP10. Interestingly, this effect was not observed in the deletion background, where levels were upregulated in the wild-type strain when compared with a Δ*sabS* deletion strain. Results observed in the Δ*sabS* deletion strain may be the most relevant, as SabS appeared to enhance translation of ABUW_RS13040-sfGFP mRNA.

In summary, differences between results in *A. baumannii* and *E. coli* indicate that SabS mediated regulation of these four mRNAs could be host dependent and that multiple mechanisms might be at play, which require further experimental investigation. All sRNA-target experiments did show molecular phenotypes, which will need further exploration. It is also noted that the results from the Δ*sigAB* background were inconsistent across kinetic assays and endpoint measurements, thus further experiments will be needed to make a conclusion on the effects of a *sigAB* deletion on expression levels of these four lipoproteins.

Since SigAB is a direct regulator of SabS, and both have shown to modulate the copper stress response (Bacon et al., 2025), both Δ*sabS* and Δ*sigAB* were tested under various stress conditions (osmotic (NaCl), membrane (SDS), and protein biosynthesis (chloramphenicol)). There was an observed growth defect in AB5075 Δ*sabS* when grown in both 0.01% and 0.03% SDS, compared with AB5075 WT. Since SDS is a known bacterial cell membrane disruptor, and many bacterial sigma factors regulate the ESR this was considered an appropriate test to gauge the role of SigAB and possibly SabS in mediating the ESR (Updegrove et al., 2016). Interestingly, this growth defect was not seen in the Δ*sigAB* strain, suggesting that SabS may play a role in envelope stress, but this is not mediated by SigAB. Considering SigAB is a direct regulator of SabS, this could infer a broader role of SabS within the AB5075 regulatory network and that its expression may be controlled by other transcription factors, too. This has been documented in other bacterial species, in *E.coli* the ESR sigma factor σ^E is a direct regulator of several documented sRNAs that regulate outer membrane homeostasis, however also exert broader regulatory roles independent of σ^E. (Coornaert et al., 2010). To fully understand the potential role of SabS in ESR mediation, future work could focus on transcriptome profiling in a SabS deletion background. Additionally, comparing this with a SigAB deletion background could further understanding of how SabS modulates stress responses independently of SigAB, despite it being a direct target for regulation by this sigma factor.

The analysis of the AB5075 RNA interactome by Hi-GRIL-seq has been previously employed , leading to discovery of 706 putative sRNA-RNA interactions (Hamrock, 2025).
In this study, this method was employed in two new conditions – late stationary phase (LSP) , and early exponential phase (EEP). Sequencing results yielded from AB5075 samples induced at LSP did not yield detectable chimeras, however several potential sRNA-RNA interactions were identified in EEP.

Enrichment of chimeras at EEP during this study yielded fewer chimeric reads compared with MEP, with 2,374 chimeric reads across induced samples, and 474 chimeric reads across non-induced samples (Hamrock, 2025). This difference could be attributed to growth-phase sensitive sRNA expression, as there is evidence of differential sRNA expression, where the expression profile of several sRNAs has shown to differ depending on growth-phase (Raad et al., 2021; Rau et al., 2015; Stubben et al., 2014). While sRNA expression is mostly studied in response to acute stress and stationary phase responses, sRNA expression in exponential phase is typically involved in nutrient transport and metabolism. Small RNAs sts132 and sts347, downregulated genes involved in aminoacyl-tRNA biosynthesis and glycolysis/gluconeogenesis in EEP in lactic acid bacteria, and sRNA GcvB represses amino acid and peptide transporters in *Salmonella* (Liu et al., 2021; C. M. Sharma et al., 2007).

A higher enrichment of reads during MEP could reflect higher sRNA gene expression during this phase of growth, possibly due to the metabolic shift during early stationary phase from exponential growth toward nutrient acquisition and stress tolerance, which is consistent with the role of many sRNAs in stress tolerance pathways (Liu et al., 2021; Navarro Llorens et al., 2010). Induction is visible across both experiments indicating that T4 RNA ligase mediated ligation occurred in both cases, and the difference in chimeric reads is more likely due to induction at EEP and MEP resulting in different sRNA profiles.

Notably, SabS was found in two mRNA containing chimeras, with OmpA family protein ABUW_RS03195, and with ABUW_RS00045. The interaction between SabS and ABUW_RS00045 has been investigated during this study, as described previously. OmpA

(outer membrane protein A) is the most abundant porin in the *A. baumannii* outer membrane. In *A. baumannii* AB5075, mutations in OmpA-like proteins have shown to increase bacterial cell membrane permeability, impact cell envelope thickness, adhesion, virulence, and motility. Furthermore, some OmpA mutants showed growth defects during exponential phase (Scribano et al., 2024). In addition to being found in chimeras with SabS, ABUW_RS03195 was found in two other putative sRNA containing chimeras, with sRNA84 and sRNA24. The presence of SabS in OmpA-like protein containing chimeras may infer a broader role of SabS in cell envelope homeostasis, since SabS deletion strains were sensitive to SDS. This phenotype was not seen in a *sigAB* deletion mutant, which could infer that SabS acts through a pathway that is at least partially independent from SigAB in regulating genes involved in envelope homeostasis.

CsrA is a widely distributed RNA - binding bacterial protein , and regulator of the Carbon Storage Regulatory (Csr) Network. CsrA represses stationary phase processes, including biofilm formation and the stringent response, while activating exponential phase processes. Regulation of CsrA is typically mediated at the protein level by inhibitory sRNAs, CsrB and CsrC, which act by sequestering CsrA and preventing binding of its targets in order to de-repress stationary phase genes (Potts et al., 2017). Interestingly, CsrA was also found in chimeras with ABUW_RS14070 (a capsule assembly Wzi family protein) and another hypothetical protein (ABUW_RS11140). Csrb mediated regulation of CsrA is well documented, however less is known about its other targets. The identification of two additional putative targets of CsrB in this dataset could infer it exerts a broader regulatory function than just repression of CsrA. Further experiments are needed to characterize the role of CsrB beyond CsrA repression, such as reporter assays or transcriptomic analysis of a Δ*csrB* mutant. sRNA81 was found in chimeras with ABUW_RS0082, a putative porin protein, and sRNA77 was found in multiple chimeras with ABUW_RS16970, an ABC transporter, suggesting a convergence of these sRNAs acting in early stationary phase to maintain envelope homeostasis.

Overall, the results from the Hi-GRIL-seq point toward sRNA mediated regulation of envelope homeostasis, and possibly regulating genes involved in envelope assembly, a trend that has been well documented in gram-negative pathogens (Yang et al., 2025b), however these interactions will need to be verified in vivo through translational reporter systems. In addition, the

identification of SabS containing chimeras with an OmpA family protein, of which have been shown to affect membrane permeability in AB5075, as well as the increased susceptibility phenotype of AB5075 *Δsabs* when grown in SDS suggests a potential role of SabS in maintaining the bacterial cell membrane.

References

Álvarez-Fraga, L., Rumbo-Feal, S., Pérez, A., Gómez, M. J., Gayoso, C., Vallejo, J. A., Ohneck, E. J., Valle, J., Actis, L. A., Beceiro, A., Bou, G., & Poza, M. (2017). Global assessment of small RNAs reveals a non-coding transcript involved in biofilm formation and attachment in Acinetobacter baumannii ATCC 17978. *PLOS ONE*, *12*(8), e0182084. https://doi.org/10.1371/journal.pone.0182084

Anderson, S. E., Chin, C. Y., Weiss, D. S., & Rather, P. N. (2020). Copy Number of an Integron-Encoded Antibiotic Resistance Locus Regulates a Virulence and Opacity Switch in Acinetobacter baumannii AB5075. *mBio*, *11*(5), e02338-20. https://doi.org/10.1128/mBio.02338-20

Bacon, E. E., Myers, K. S., Iruegas-López, R., Banta, A. B., Place, M., Ebersberger, I., & Peters, J. M. (2025). Physiological roles of an *Acinetobacter* -specific σ factor. *mBio*, *16*(6), e00968-25. https://doi.org/10.1128/mbio.00968-25

Bostanghadiri, N., Narimisa, N., Mirshekar, M., Dadgar-Zankbar, L., Taki, E., Navidifar, T., & Darban-Sarokhalil, D. (2024). Prevalence of colistin resistance in clinical isolates of Acinetobacter baumannii: A systematic review and meta-analysis. *Antimicrobial Resistance & Infection Control*, *13*(1), 24. https://doi.org/10.1186/s13756-024-01376-7

Carrier, M.-C., Lalaouna, D., & Massé, E. (2016). A game of tag: MAPS catches up on RNA interactomes. *RNA Biology*, *13*(5), 473–476. https://doi.org/10.1080/15476286.2016.1156830

Casella, L. G., Weiss, A., Pérez-Rueda, E., Antonio Ibarra, J., & Shaw, L. N. (2017). Towards the complete proteinaceous regulome of Acinetobacter baumannii. *Microbial Genomics*, *3*(3). https://doi.org/10.1099/mgen.0.000107

Coyne, S., Courvalin, P., & Périchon, B. (2011). Efflux-Mediated Antibiotic Resistance in *Acinetobacter* spp. *Antimicrobial Agents and Chemotherapy*, *55*(3), 947–953. https://doi.org/10.1128/AAC.01388-10

Da Silva, G., & Domingues, S. (2016). Insights on the Horizontal Gene Transfer of Carbapenemase Determinants in the Opportunistic Pathogen Acinetobacter baumannii. *Microorganisms*, *4*(3), 29. https://doi.org/10.3390/microorganisms4030029

Dehbanipour, R., & Ghalavand, Z. (2022). *Acinetobacter baumannii*: Pathogenesis, virulence factors, novel therapeutic options and mechanisms of resistance to antimicrobial agents with emphasis on tigecycline. *Journal of Clinical Pharmacy and Therapeutics*, *47*(11), 1875–1884. https://doi.org/10.1111/jcpt.13787

Doi, Y., & Arakawa, Y. (2007). 16S Ribosomal RNA Methylation: Emerging Resistance Mechanism against Aminoglycosides. *Clinical Infectious Diseases*, *45*(1), 88–94. https://doi.org/10.1086/518605

Evans, B. A., & Amyes, S. G. B. (2014). OXA β-Lactamases. *Clinical Microbiology Reviews*, *27*(2), 241–263. https://doi.org/10.1128/CMR.00117-13

Georg, J., Lalaouna, D., Hou, S., Lott, S. C., Caldelari, I., Marzi, S., Hess, W. R., & Romby, P. (2020). The power of cooperation: Experimental and computational approaches in the functional characterization of bacterial sRNAs. *Molecular Microbiology*, *113*(3), 603–612. https://doi.org/10.1111/mmi.14420

Gottesman, S., & Storz, G. (2011). Bacterial Small RNA Regulators: Versatile Roles and Rapidly Evolving Variations. *Cold Spring Harbor Perspectives in Biology*, *3*(12), a003798–a003798. https://doi.org/10.1101/cshperspect.a003798

Hamrock, F. J., Guest, T., Daum, M. N., Connell, O., Ershova, A. S., Hokamp, K., Fleming, A. B., Gebhardt, M. J., Westermann, A. J., & Kröger, C. (2025). *DNA uptake and twitching motility are controlled by the small RNA Arp through repression of pilin translation in* Acinetobacter baumannii. Microbiology. https://doi.org/10.1101/2025.07.19.665661

Hoekzema, M., Romilly, C., Holmqvist, E., & Wagner, E. G. H. (2019). Hfq-dependent mRNA unfolding promotes sRNA -based inhibition of translation. *The EMBO Journal*, *38*(7), e101199. https://doi.org/10.15252/embj.2018101199

Hör, J., Gorski, S. A., & Vogel, J. (2018). Bacterial RNA Biology on a Genome Scale. *Molecular Cell*, *70*(5), 785–799. https://doi.org/10.1016/j.molcel.2017.12.023

Howard, A., O'Donoghue, M., Feeney, A., & Sleator, R. D. (2012). Acinetobacter baumannii: An emerging opportunistic pathogen. *Virulence*, *3*(3), 243–250. https://doi.org/10.4161/viru.19700

Jawad, A., Seifert, H., Snelling, A. M., Heritage, J., & Hawkey, P. M. (1998). Survival of *Acinetobacter baumannii* on Dry Surfaces: Comparison of Outbreak and Sporadic Isolates. *Journal of Clinical Microbiology*, *36*(7), 1938–1941. https://doi.org/10.1128/JCM.36.7.1938-1941.1998

Kröger, C., MacKenzie, K. D., Alshabib, E. Y., Kirzinger, M. W. B., Suchan, D. M., Chao, T.-C., Akulova, V., Miranda-CasoLuengo, A. A., Monzon, V. A., Conway, T., Sivasankaran, S. K., Hinton, J. C. D., Hokamp, K., & Cameron, A. D. S. (2018). The primary transcriptome, small RNAs and regulation of antimicrobial resistance in Acinetobacter baumannii ATCC 17978. *Nucleic Acids Research*, *46*(18), 9684–9698. https://doi.org/10.1093/nar/gky603

Kyriakidis, I., Vasileiou, E., Pana, Z. D., & Tragiannidis, A. (2021a). Acinetobacter baumannii Antibiotic Resistance Mechanisms. *Pathogens*, *10*(3), 373. https://doi.org/10.3390/pathogens10030373

Liao, X., Ma, Y., Daliri, E. B.-M., Koseki, S., Wei, S., Liu, D., Ye, X., Chen, S., & Ding, T. (2020). Interplay of antibiotic resistance and food-associated stress tolerance in foodborne pathogens. *Trends in Food Science & Technology*, *95*, 97–106. https://doi.org/10.1016/j.tifs.2019.11.006

Marotta, J., Zhao, A., Rather, P. N., & Grabowicz, M. (2025). The BfmRS stress response protects *Acinetobacter baumannii* against defects in outer membrane lipoprotein biogenesis. *Journal of Bacteriology*, *207*(1), e00332-24. https://doi.org/10.1128/jb.00332-24

Miller , W. R., & Arias, C. A. (2024). ESKAPE pathogens: Antimicrobial resistance, epidemiology, clinical impact and therapeutics. *Nature Reviews Microbiology*, *22*(10), 598–616. https://doi.org/10.1038/s41579-024-01054-w

Mogre, A., Connell, O., White, J., Shaibah, A., Hokamp, K., Hamrock, F. J., Schauer, K., & Kröger, C. (2025). Development of two compatible plasmids to assess sRNA-mediated post-transcriptional regulation in Acinetobacter baumannii. *bioRxiv*, 2025.07.11.664372. https://doi.org/10.1101/2025.07.11.664372

Moon, K., Six, D. A., Lee, H., Raetz, C. R. H., & Gottesman, S. (2013). Complex transcriptional and post-transcriptional regulation of an enzyme for lipopolysaccharide modification. *Molecular Microbiology*, *89*(1), 52–64. https://doi.org/10.1111/mmi.12257

Novović, K., & Jovčić, B. (2023). Colistin Resistance in Acinetobacter baumannii: Molecular Mechanisms and Epidemiology. *Antibiotics*, *12*(3), 516. https://doi.org/10.3390/antibiotics12030516

Pulvermacher, S. C., Stauffer, L. T., & Stauffer, G. V. (2009). Role of the sRNA GcvB in regulation of cycA in Escherichia coli. *Microbiology*, *155*(1), 106–114. https://doi.org/10.1099/mic.0.023598-0

Schilling, D., Findeiß, S., Richter, A. S., Taylor, J. A., & Gerischer, U. (2010). The small RNA Aar in Acinetobacter baylyi: A putative regulator of amino acid metabolism. *Archives of Microbiology*, *192*(9), 691–702. https://doi.org/10.1007/s00203-010-0592-6

Sharma, R., Arya, S., Patil, S. D., Sharma, A., Jain, P. K., Navani, N. K., & Pathania, R. (2014). Identification of Novel Regulatory Small RNAs in Acinetobacter baumannii. *PLoS ONE*, *9*(4), e93833. https://doi.org/10.1371/journal.pone.0093833

Sharma, R., & Lakhanpal, D. (2025). Acinetobacter baumannii: A comprehensive review of global epidemiology, clinical implications, host interactions, mechanisms of antimicrobial resistance and mitigation strategies. *Microbial Pathogenesis*, *204*, 107605. https://doi.org/10.1016/j.micpath.2025.107605

Shenkutie, A. M., Gebrelibanos, D., Yao, M., Bedada Hundie, G., Chow, F. W. N., & Leung, P. H. M. (2023). Impairment of novel non-coding small RNA00203 inhibits biofilm formation and reduces biofilm-specific antibiotic resistance in Acinetobacter baumannii. *International Journal of Antimicrobial Agents*, *62*(3), 106889. https://doi.org/10.1016/j.ijantimicag.2023.106889

Waters, L. S., & Storz, G. (2009). Regulatory RNAs in Bacteria. *Cell*, *136*(4), 615–628. https://doi.org/10.1016/j.cell.2009.01.043

Weiss, A., Broach, W. H., Lee, M. C., & Shaw, L. N. (2016). Towards the complete small RNome of Acinetobacter baumannii. *Microbial Genomics*, *2*(3). https://doi.org/10.1099/mgen.0.000045

Woods, E. C., & McBride, S. M. (2017). Regulation of antimicrobial resistance by extracytoplasmic function (ECF) sigma factors. *Microbes and Infection*, *19*(4–5), 238–248. https://doi.org/10.1016/j.micinf.2017.01.007

Yu, J., & Schneiders, T. (2012). Tigecycline challenge triggers sRNA production in Salmonella enterica serovar Typhimurium. *BMC Microbiology*, *12*(1), 195. https://doi.org/10.1186/1471-2180-12-195

Zhang, Y., Han, K., Chandler, C. E., Tjaden, B., Ernst, R. K., & Lory, S. (2017). Probing the sRNA regulatory landscape of *P. aeruginosa*: Post-transcriptional control of determinants of pathogenicity and antibiotic susceptibility. *Molecular Microbiology*, *106*(6), 919–937. https://doi.org/10.1111/mmi.13857

Zhang, Y., Werling, U., & Edelmann, W. (2012). SLiCE: A novel bacterial cell extract-based DNA cloning method. *Nucleic Acids Research*, *40*(8), e55–e55. https://doi.org/10.1093/nar/gkr1288

Zhu, Q., Fan, Z., Zeng, L., Li, C., Ye, C., & Zheng, R. (2024). Effect of sodium dodecyl sulfate (SDS) on microbial community structure and function in lake–terrestrial ecotones: A simulation experiment. *Environmental Technology & Innovation*, *34*, 103594. https://doi.org/10.1016/j.eti.2024.103594